LASER & PHOTONICS REVIEWS

Laser Photonics Rev. **6**, No. 4, 564–587 (2012) / **DOI** 10.1002/lpor.201100044

Abstract This review article is concerned with basic aspects and some selected topics in photonic crystal (PhC) devices. It starts with a significantly historical aspect of basic principles for photonic crystals that it is hoped will help the reader to develop a critical appreciation of the research literature. It continues by describing topics such as PhC beamsplitters, slow-light structures, micro-/nanoresonators, coupled resonator optical waveguides (CROWs) and PhC-based semiconductor lasers. Emphasis is placed on both the conceptual and the practical matters that need to be addressed in order to fulfill the tasks of designing and realizing devices that exploit photonic crystal principles. The review also addresses some of the problems encountered in the fabrication of photonic crystal devices using the planar technologies of integrated photonics, which are those that are most likely to be used in future commercial production.

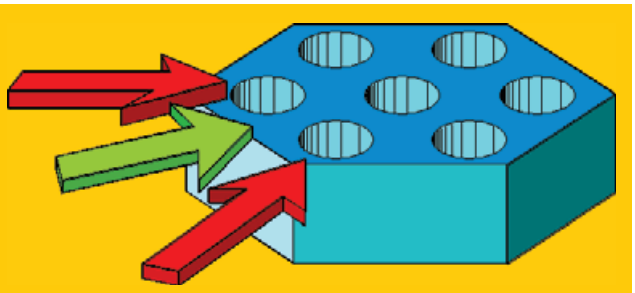

Photonic crystal devices: some basics and selected topics

Richard M. De La Rue[1,2,*] **and Christian Seassal**[3]

1. Introduction

Before embarking on a review of the topic of photonic crystal devices, it is appropriate to consider briefly what is generally understood by the words 'photonic crystal' (PhC) and the closely associated combination of words 'photonic bandgap' (PBG). It is not our intention, in the present article, to provide a detailed history related to these expressions – and how they came to be coined. But it is still appropriate to mention the seminal papers of Yablonovitch [1] and John [2], as well as the earlier work of Bykov [3], because of the direct connections between the concepts set out in the papers by these three authors and the concepts employed in applicable photonic crystal device structures.

In his seminal paper published in 1987, Yablonovitch [1] was particularly concerned with the possibility that the light-emission process could be greatly modified, i. e. filtered, by forming the emitting material into a three-dimensionally periodic structure. Crucially, he recognized that strongly contrasting alternate regions of 'high' and 'low' refractive index were required, in the emitting medium. Yablonovitch also recognized that the refractive index of the material should alternate periodically on a distance scale that was comparable with half of the wavelength of light in the composite medium, so that strong *Bragg reflection* effects would occur. He further recognized that such periodic structures might even inhibit the propagation of light through the medium to such an extent that it would become, in principle, impossible for light – in an appropriately chosen range of wavelengths – to propagate in any direction. This possibly omnidirectional stop-band behavior could be understood as providing a conceptual analogy between the behavior of light ('*photons*') in a medium with a periodic variation in its refractive index and the behavior of *electrons* in single-crystal semiconductors. It should be said immediately that the behavior of the light in these circumstances is a wave-propagation phenomenon and a kind of generalized Bragg diffraction, rather than a form of photon (i. e. particle-like) behavior.

A key aspect of the paper by Yablonovitch was the motivation to reduce the threshold 'pump' level for laser operation in an optical gain medium. Below the threshold level for lasing, light emission is predominantly a spontaneous process – whereas, above threshold, light emission is predominantly a stimulated process. As the acronym '*light amplification by stimulated emission of radiation*' (LASER) clearly implies, what is sought in reducing the threshold for laser action is a reduction in the pump level at which the optical gain medium makes the transition from predominantly *spontaneous* emission to predominantly *stimulated* emission. The inhibition of the escape of spontaneously emitted photons that is characteristic of media with photonic stop-band properties has the direct consequence of increasing the level of stimulated emission for a given pump level – and therefore implies a reduction in the threshold. Bykov's [3] significantly earlier work was concerned with *distributed feedback* (DFB) laser action. DFB lasers with one-dimensionally periodic gratings embedded in an epitaxially grown, heterostructure, semiconductor gain-medium are the life-blood light sources of large-bandwidth, long-haul, fiber-optical communication systems. But Bykov's important contribution, from our present point of view, was the recognition that the threshold for laser action could in principle be greatly reduced through the imposition of strong refractive index periodicity in all three space dimensions, thereby addressing the intrinsically omnidirectional nature of spontaneous emission. Bykov recognized that the

[1] Photonics Research Centre, Physics Department, Science Faculty, University of Malaya, 50603 Kuala Lumpur, Malaysia [2] Optoelectronics Research Group, School of Engineering, University of Glasgow, Rankine Building, Oakfield Avenue, Glasgow G12 8LT, Scotland, UK [3] Institut des Nanotechnologies de Lyon, UMR CNRS 5270, Ecole Centrale de Lyon, 36 avenue Guy de Collongue, 69134 Ecully Cedex, France
[*] Corresponding author: e-mail: richard.delarue@gla.ac.uk

immediate consequence of creating a three-dimensionally periodic DFB structure within a gain medium could be a large reduction in the laser threshold. Complete inhibition of spontaneous emission in almost all directions in a solid gain medium, together with the existence of 'defect states' in the form of a narrow angular cone of permitted light propagation, leads to a greatly reduced lasing threshold.

2. Semiconductors of light

The phrase 'semiconductors of light' has been used (Yablonovitch [4]) when considering the nature of photonic crystals and the possibility of their demonstrating photonic bandgap behavior – and it correctly evokes analogous behavioral concepts that are valid and applicable. Just as is the case of conduction by electrons in semiconductors, photonic crystals exhibit distinct regions of the frequency (i. e. equivalently, photon energy) spectrum in which the propagation of light is strongly inhibited. The frequency (energy) range covered by these stop-bands depends on the choice of direction, with respect to the defining axes of the photonic crystal. With sufficiently large variation in the periodic refractive index – and the correct distribution of this changing refractive index – full photonic bandgap (PBG) behavior occurs. More generally, the behavior of light in photonic crystals is characterized by band structure, just as is the case for the electronic properties of semiconductors. Moreover, concepts from solid-state theory such as *densities of states* are useful in describing both the optical properties of photonic crystals and the electronic properties of semiconductors.

But the nature of the propagation of *coherent* light, in and through a medium with a periodic refractive index variation, is *not* the same as that of electrical current flowing through a semiconductor, except possibly for the situation of very low temperature conditions in the semiconductor. Nor is there an obvious analogy between photonic bandgap (PBG) properties and the possibility of *electrical conduction* by *holes*, when an electric field is produced in a semiconducting medium. The physically significant point here is that – in the usual conditions that apply from above room temperature down to nearly absolute zero – the electronic band structure of a crystalline semiconductor implies that electrons in the conduction band of the semiconductor are accelerated, i. e. they gain energy, in an applied electric field – but only during a very brief period of time before a random scattering event occurs, caused by one of several different possible processes. The important scattering processes available for electrons (and holes) in semiconductors include phonon scattering, defect scattering, impurity scattering and carrier–carrier scattering. The repeated acceleration and deceleration of conduction electrons (and conceptually the same process for 'holes') under the influence of an electric field is, of course, the familiar process of charge-carrier *drift*. Electrical conduction by the drift mechanism is characteristically an *incoherent* process. While coherent *electronic* propagation in solid media is experimentally possible, the conditions under which it can be observed are typically quite extreme, requiring high-purity material, very low defect density and extreme cryogenic (e. g. milliKelvin) temperatures. Of course, optical waves (and electromagnetic waves more generally) are also susceptible to scattering processes – and processes such as *Raman scattering* and *Brillouin scattering* are associated with a rich body of experimental physics. Both of these processes, in the quantum (particle) language that is now appropriate, involve interactions between photons and *phonons* – and lead to changes in the frequency (wavelength) of some of the light involved. Wave–particle duality implies, in such scattering processes, that there is an equivalence between the conservation of (particle) *momentum* and *energy* – and the *frequencies* of the waves involved and the direction and magnitude of their *propagation constants*.

Rayleigh scattering of light occurs in all real media, because of the presence of imperfections (on various size scales) and associated local fluctuations in the refractive index – and additionally because of irregularities (i. e. roughness) at surfaces and interfaces. Because the scatterers involved in the Rayleigh scattering process are essentially unmoving, the light that is scattered does not undergo frequency or wavelength shifting. The result of coherent but random scattering may, in appropriate circumstances, be identified as the phenomenon of *speckle*. In the context of photonic crystal (PhC) structures, which intrinsically are characterized by a general version of strong Bragg scattering, the inevitable presence of Rayleigh scattering becomes a source of propagation loss – but also the origin of a version of speckle that takes the form of significant dephasing of the optical propagation. Randomness in the position, size and shape of the ostensibly regular elements that form the photonic crystal structure can be considered as generating particular forms of Rayleigh scattering.

Later in this article, we shall consider the interesting topic of *slow light* in photonic crystal (PhC) structures – and we shall note how slow light is characteristically more strongly affected by Rayleigh scattering than faster light. Having mentioned the topic of slow light – and the fact that scattering losses are enhanced by slowing propagation, we immediately cite the work of Patterson et al. [5, 6] – and Mazoyer et al. [7] as examples of significant recent papers in the literature on the propagation losses associated with slowing of optical propagation.

3. Anderson localization and slow light

John's equally seminal paper [2] on strong localization in photonic crystals appeared almost immediately after that of Yablonovitch – and in the same journal. Moreover, the connection between these two papers was established immediately through John's citation of the slightly earlier paper by Yablonovitch. John was concerned with the electromagnetic properties of 'disordered dielectric superlattices'. He proposed that the well-known (but experimentally very difficult to demonstrate) phenomenon of 'Anderson localization' [8] for electrons in semiconductors – or for magnetic

spin lattices – might be observable – and more easily – for electromagnetic waves in periodic structures.

The reader may be somewhat surprised by the appearance of a phrase (*Anderson localization*) that is frequently used by physicists concerned with the propagation and scattering of waves in periodic structures. That phrase comes from fundamental considerations of the electronic band structure of solid materials – and, in particular, from the possible impact of disorder in what is otherwise a regularly periodic medium such as a single crystal of a semiconductor like silicon. The original work by P. W. Anderson, published in Physical Review in 1958, on localization of spin states or of electrons led directly to the subsequent award, in 1977, of the Nobel prize in physics. It is hard to overstate the conceptual importance of Anderson's prediction of the possibly strong, but uncontrolled, effects on the transmission spectrum that result from small imperfections in periodic structures. The phenomenon of Anderson localization results directly from the interference of multiple waves, once the possibility of deviation from pure periodicity is contemplated. *Anderson localization* describes a situation where, at some specific frequency, deviations from perfect spatial periodicity in the 'crystal' lead to the (electromagnetic) energy in the system not being evenly (but periodically) distributed. Instead, the modal energy becomes concentrated in a finite region of the crystal. This behavior is much the same as that of forming a microcavity region accidentally in the neighborhood of an unintended defect in the periodic lattice.

In the paper written by Anderson, the question posed was whether there might be circumstances in which the normal transport of excitations in a solid, of which one example is electronic charge carriers, might be significantly disturbed by localization effects. Taking disorder in a reasonably general sense, it can be said that the impact of various types of disorder is a central issue for photonic crystal devices. This assertion applies whether the disorder is a deliberately added one, with a specific spatial configuration and physical properties, or the disorder is an intrinsic aspect of how the photonic crystal structure has been formed. The possibility, indeed inevitability, of Anderson localization is a matter of real *engineering* concern in photonic crystal devices.

The paper by John [2] is important: an assertion that is emphasized in the perspective of more recent work in which radically slow (i. e. low group velocity) light propagation has been observed – or microcavities have been formed – in photonic crystal structures. The paper is seminal because it is both implicitly and explicitly concerned with how the propagation of light is determined by periodic structuring of a medium and how that propagation can be radically modified – and impeded – by the presence of defect states. It also connects directly with the high quality factor (Q-factor) planar-waveguide-based PhC microcavities that have now been demonstrated.

4. Device effects

Photonic crystals may be considered as forming a general version of a diffraction grating. Provided that the propagation path through a periodic structure is sufficiently large, the scattering of light is intrinsically a form of Bragg scattering. Even for a structure that is periodic along only a single direction, the basic rules of energy and momentum conservation apply. Energy conservation, for the interaction of light with a static grating, implies that the Bragg-scattered light does not undergo any shift in its frequency. Because momentum is a vectorial quantity, there is the fundamental possibility that the Bragg-scattered light will propagate in a direction that is – or directions that are – quite different from the initial direction of optical propagation. For photonic crystal structures that are embedded in a finite thickness waveguide layer, the interaction of a guided light beam with the photonic crystal structure may generate both guided-light Bragg-scattering and out-of-plane Bragg-scattered light.

Periodic variation in the electromagnetic properties of a medium leads intrinsically to the occurrence of band structure, i. e. to dispersive propagation in which the phase velocity varies with frequency according to the periodicity of the medium and the spatial and frequency dependence of the properties of the medium. Permitted modes of propagation of light in periodic media are called Bloch waves and, in general they have the same periodicity as the medium, together with higher space harmonics of the fundamental periodicity [9–11].

The fact that a periodic variation in the refractive index leads to Bragg stop-band behavior intrinsically provides the possibility of exploiting planar PhC structures for the realization of spectral filter devices. The demonstration of a close approximation to an omnidirectional stop-band, i. e. photonic bandgap (PBG) behavior, leads to the possibility of device effects such as channel waveguide confinement, when a suitable defect structure is formed. The channel waveguide can be produced conceptually by removing one or more rows of the basic elements (e. g. holes in a solid medium) along a high-symmetry direction of the photonic crystal lattice, e. g. one row, to form a W1 channel waveguide. More generally, a channel waveguide can conceptually be produced by the relative lateral displacement of two distinct blocks of a photonic crystal lattice with respect to each other, thereby giving waveguides that can be labelled as, e. g., W0.7 or W1.3 [12, 13].

The channel waveguide is only one possible example of a PhC defect structure that is useful in devices. In terms of the related band structure, the modes of propagation in channel waveguides in a PhC lattice will exhibit characteristic *additional* dispersion curves in $\omega - \mathbf{k}$ space, along the direction of the waveguide axis – and there will be associated ministopbands. Microcavities formed by removing a finite number of holes from a lattice also produce defect states or modes that are nonpropagating. We make the point that many devices realized within a PhC environment are characteristically associated with the creation of defects in the PhC lattice – and that device engineering (i. e. design) involves a selective exploration of all the possible deformations of the lattice that can be imagined, e. g. changes in hole size, position, shape and orientation, in a hole-based PhC lattice. The simple conceptual change from a purely circular hole elemental shape in a 2D periodic lattice to an elliptical ele-

mental shape that might be rotated inplane can have a useful impact on device properties, e. g. for slow-light propagation in channel waveguides [14].

Although the most general case of a PhC structure observed in '3-space' is a three-dimensionally periodic lattice (possibly with three distinct 'orthogonal' axes defining the positions of the elements forming the lattice – and three different periodicities along these axes), a large fraction of the effects associated with the presence of photonic crystal structuring can be understood by examining the effect of periodicity in a two-dimensionally periodic structure, thereby neglecting the third dimension. Strictly speaking, this last statement is an oversimplification – since the variation of the refractive index in the direction that is normal to the planes of 2D periodicity impacts more-or-less strongly on the Bragg-scattering process. Figure 1 shows, schematically, part of a region of 2D periodic photonic crystal in a planar optical waveguide layer. In passing, we note that, just as with real crystals defined at the atomic level, the concepts of both point-group symmetry and space-group symmetry are applicable in the general photonic crystal structure, whether it has 3D or 2D periodicity.

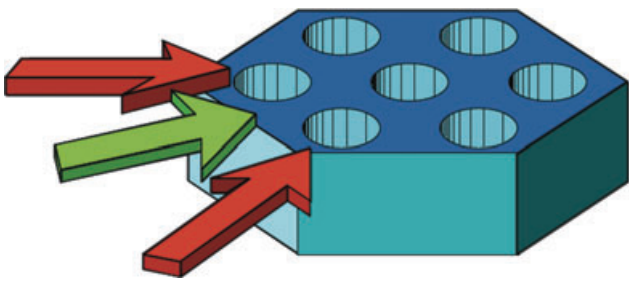

Figure 1 (online color at: www.lpr-journal.org) Schematic representation of part of a 2D-periodic photonic crystal structure formed by cylindrical 'air' holes in a solid waveguide layer, based on a diagram originally generated by T. F. Krauss. The outer two arrows indicate equivalent major propagation directions (red color online) that apply for a 'triangular' lattice with hexagonal, six-fold, rotational symmetry. The single inner arrow (green online) indicates the direction that is exactly half-way in-between – and has the most strongly differentiated propagation properties.

For the case where the photonic crystal structure is only periodic in '2-space' – and it is embedded in a planar waveguide, the modes of propagation may be classified as either guided modes or radiation modes. A single high(-er) refractive index layer, with holes arranged periodically in it, may only exhibit radiative Bloch modes, because the layer is too thin. But coupling to and from these radiative Bloch modes may exhibit very sharply resonant behavior [15].

Even with lattices made up from completely isotropic building blocks, i. e. circular cylinders, a 2D periodic array of light scatterers potentially gives rise to several interesting phenomena (behavior/characteristics) that may be exploited in photonic devices. The band structure of a two-dimensionally periodic photonic crystal (PhC) lattice can, with a sufficiently large refractive index contrast and the right choice of the ratio of cylinder diameter to lattice spacing lead to the phenomenon of a full photonic bandgap (PBG). The existence of a full PBG implies that there is a stop-band for light propagation in all directions within the defining plane of the lattice – and, strictly, for all possible polarization (electromagnetic field orientation) conditions. More practically [16], a full PBG can be obtained for light with a single polarization condition – defined by the 'TE' mode of a planar thin-film waveguide with a suitably high refractive index. We remark here that some commercial electromagnetic computational software labels the 'TE' modes in photonic crystal modeling problems as the 'TM' modes – e. g. in 2D photonic crystal lattices formed in planar waveguides. This unnecessary confusion arises primarily from the need to define and compute an appropriate value for the *effective* refractive index of the waveguide layer. It should also be clearly understood that the 'TE' modes here are ones in which the main electric-field component of the propagating light is parallel to the waveguide plane – and that the PhC Bloch modes, whether or not they are fully confined waveguide modes, are strictly *hybrid* modes, for the general case of an arbitrary inplane propagation direction. The Bloch modes of 2D PhC structures embedded in planar waveguides are, in this general situation, more accurately labelled as 'quasi-TE' or 'quasi-TM'.

The detailed behavior of light propagating through the two-dimensionally periodic PhC lattice typically varies strongly with the choice of propagation direction. Group velocity and phase velocity are, in general, only collinear along 'high-symmetry' directions – and particular choices of the propagation conditions (i. e. the initial choice of the propagation direction and the normalized frequency) may lead to the strong 'beam-steering' effects that have been exploited in PhC-based 'superprisms'. Other interesting phenomena may be observable, such as low (in principle, as low as zero) group velocity, large (possibly infinite) phase velocity, negative refraction and backward waves. We shall treat some of these phenomena in more detail, later in the present review.

5. Rods (pillars) versus holes

Until recently, *experimental* research on planar-waveguide-based photonic crystal device structures has been almost universally based firmly on the use of 'air' holes in a 'high' refractive index waveguide core layer. For some purposes, it has been considered practically essential that the basic planar waveguide take the form of a thin suspended membrane made from a transparent, but high refractive index, layer of a semiconductor such as silicon ($n \sim 3.5$) that is completely and symmetrically (in the 'vertical' direction) immersed in air. A specific value for the silicon membrane waveguide thickness that has become a de facto standard is (nominally) 220 nm. This particular choice is not essential – and viable device structures can be realized with both somewhat thicker and somewhat thinner waveguide core thicknesses. Vertical symmetry is also not an absolute requirement – and potentially viable device performance can

be obtained, for instance, with a high-index silicon waveguide core supported by a silica ($n \sim 1.45$) lower cladding layer, with air above the waveguide core layer – as well as in the holes in the high index core. Because of the smaller refractive index difference for a silicon waveguide core layer supported by (or both supported and covered by) silica, the thickness of the silicon core layer may be much larger. As an example, a 470-nm thick silicon core layer can provide viable guided, i. e. nonleaky, photonic crystal Bloch modes when supported by a silica lower cladding layer, with air above the waveguide core layer [14].

In contrast to the situation for optical frequency experimental work, much of the theoretical analysis and modeling of two-dimensionally periodic photonic crystal structures has been based on lattices (often 'square' lattices) of rods or pillars with a high refractive index, immersed in air. Modeling such lattices of cylindrical rods without consideration of the third ('vertical') dimension is equivalent to the assumption of rods that are infinite along the third dimension, so that the practical issue of confinement along this direction does not arise.

In times past, the disconnection between the *computational modeling* of rod-based PhCs and the experimental realization of PhC structures based on holes in waveguides was sufficiently large that the experimental researcher could safely ignore a large part of the body of results obtained theoretically by computational modeling of the rod-based PhCs. This somewhat complacent situation has been substantially changed by two distinct developments:

a) The realization of high aspect ratio pillar-based photonic crystal beamsplitters and microcavity sensors in relatively thick amorphous silicon films [17, 18]. Despite the intrinsically leaky character of the finite height (length) rod-based 2D PhC, quite impressive and practically sufficient performance can be delivered – with resonance Q-factor values greater than 20 000 being demonstrated.
b) The quantum cascade (QC) laser with 2D PhC Bragg mirrors, as described by Walker and coworkers [19] and Hvozdara and coworkers [20]. The QC laser may yet 'rescue' the basic PhC laser concept set out by Bykov [3] and Yablonovitch [4], since its unipolar carrier operation renders it intrinsically much less vulnerable to the massively efficiency reducing impact of nonradiative processes. These are the processes that mar the performance of the standard diode injection lasers that function through hole–electron recombination. The vertical confinement properties of typical QC laser structures [19, 20] are also favorable for the rod-in-air 2D PhC configuration.

6. Photonic crystal beamsplitters

The use of photonic crystal structures to perform the beamsplitting operation in planar waveguides has received much attention [17, 21–30] – and promising results have been obtained. For the present authors, a beamsplitter is a device that produces at least two distinct beams of light in different directions at exactly the same wavelength as that of a single beam of light that is incident on the beamsplitting device.

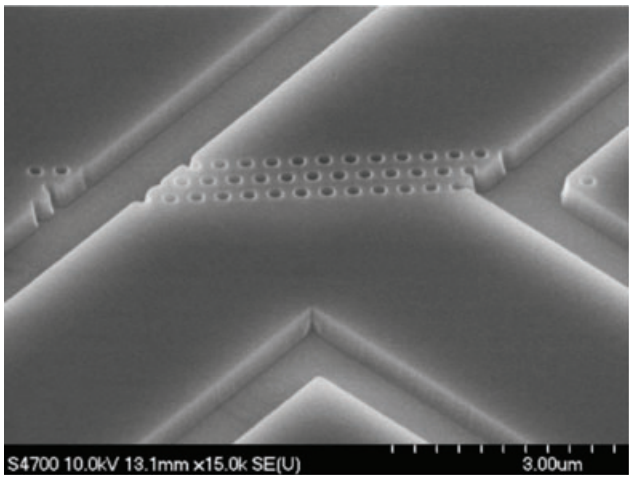

Figure 2 Scanning electron micrograph of polarization selective PhC beamsplitter on SOI ridge-waveguide T-junction. Image extracted, with permission, from [21].

Our strong preference is to use the word *beamsplitter* only for photonic devices that operate on wide, well-collimated, light beams where transverse confinement is a minimal feature of operation or else is nonexistent. We therefore exclude from consideration, in the present context, papers in the literature that use the word beamsplitter to describe power-dividing devices in which the incident light beam and the separated output beams are, for instance, confined (strongly) in photonic crystal channel waveguides [31, 32].

Beamsplitters for controlled power division of light having a single polarization – or for controlled polarization separation and selection in photonic integrated circuits (PICs) [22] – have been realized using air-hole, 1D or 2D, PhC structures in relatively wide semiconductor ridge waveguides. Such realization has been typically achieved in compact configurations that occupy areas of only a few square micrometers. An obvious question is: 'What does a photonic crystal beamsplitter look like?' Figure 2 (taken from [21]) shows a scanning electron micrograph of a specific example of a 2D PhC based beamsplitter, embedded in a silicon-on-insulator (SOI) waveguide. The structure shown has three rows of holes in a triangular lattice that, in the wavelength range of interest (around 1500 nm), has a stop-band for the propagation of TE light, which is therefore largely reflected by the finite width photonic crystal region. Because of the symmetry of the interaction configuration, with the three rows of holes being oriented at 45 degrees with respect to the light beam arriving along the waveguide axis, the 'reflected' beam propagates at right angles to the incident beam – and therefore exits via the right-hand arm of the 'wide' ($\sim 3\,\mu$m) waveguide T-junction in which the photonic crystal beamsplitter pattern is embedded. It should be stressed that the apparently reflective behavior is strictly one of directional diffraction – and implies a specific choice of the PhC lattice constant and hole diameter.

In contrast to the situation just described, which applies for TE-polarized light, the photonic crystal region that forms a nominally complete reflector for the TE-polarized light

does not exhibit a stop-band for TM-polarized light. This particular beamsplitter structure is therefore a polarization-sensitive device – and performs the potentially useful function of polarization separation. Polarization separation can be used as a core ingredient in a strategy that achieves polarization-independent behavior by separating the two basic polarizations (TE and TM) for operations such as electro-optic modulation – for which the control voltage required is typically quite different for the two different polarizations. The two beams may then be recombined in a second beamsplitting structure, after the same time-dependent modulation level has been imposed in each case.

Figure 3, also taken from [21], shows a structure that uses a single, nominally uniform, row of holes in a straight line. The row of holes has been placed at an angle that bisects a right-angled T-junction of relatively wide waveguides realized in SOI. The power-splitting ratio and the polarization selectivity of this simple beamsplitter structure, at a specific wavelength, depend on both the diameter of the holes etched through the silicon core and on their spacing.

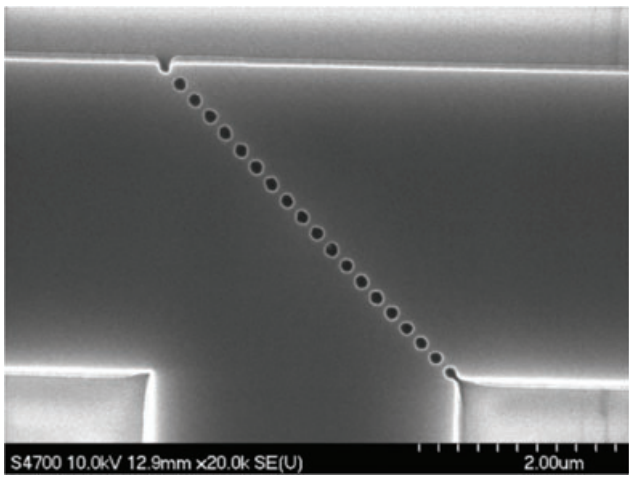

Figure 3 Beamsplitter structure formed by a single row of holes placed in a right-angled waveguide T-junction. Image extracted, with permission, from [21].

Using 3D FDTD simulation, an efficiency of more than 99% has been predicted for the case of the power splitter in a single optical polarization, with a substantial amount of freedom of choice of the power-splitting ratio between the two output branches. Measurements carried out on structures realized in waveguides on SOI resulted in an estimated global efficiency of about 95% and were in close agreement with simulations. Figure 4 is a visualization of the interaction of a (moderately) wide guided light beam with a single-row PhC beamsplitter.

The work of Pottier and coworkers [21] followed on logically from previous work by Nordin, Kim and coworkers [22–25], but differs on the significant point that Pottier et al. [21] have used the more widely accepted experimental configuration of *hole-based* PhCs. Additionally, Pottier and coworkers have used a hexagonal (triangular) lattice, rather than a square lattice. In their 2002 paper [22], Nordin, Kim

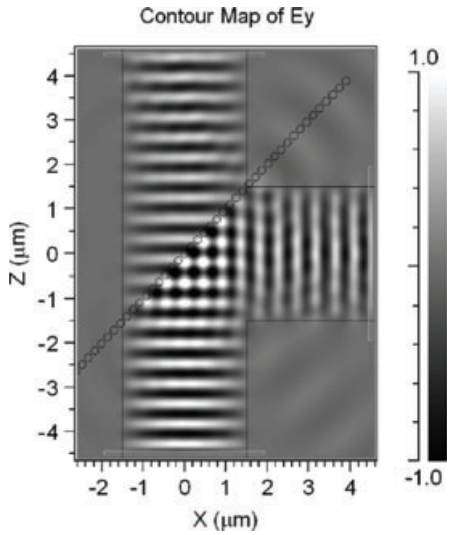

Figure 4 Simulation of a light beam in a wide channel waveguide as it encounters a single row PhC beamsplitter embedded in a wide-waveguide T-junction structure. Image extracted, with permission, from [21].

and coworkers considered both the use as beamsplitters of triangular-shaped regions of square-lattice PhCs of silicon posts in air – and both single-row and double-row PhC regions. It is important to note that the structure was modeled only in a 2D format that neglected the possibly large effect of having only a finite extension of the PhC lattice in the vertical direction. Moreover, the light was modeled as arriving and leaving in 2-μm wide waveguides with weak lateral confinement and a core refractive index value of 1.5. With the restriction of analyzing operation only for TM-polarized light (i. e. light having its electric field entirely parallel to the axes of the pillars), useful performance could be obtained both from the corner reflectors and from the beamsplitters, with the appropriate choice of lattice constant and filling factor.

A natural further step towards integration and greater complexity is to form a Mach–Zehnder structure by using two corner reflectors and two beamsplitters in the arrangement shown in Fig. 5, also taken from [22].

In their subsequent work, which has concerned corner reflectors, bends and beamsplitter structures, Li, Kim, Nordin et al. [23, 24] have modeled the use of finite, but relatively thick (in the sense of volume holography) regions of 2D PhC to provide a polarizing beamsplitter action, with the 2D PhC lattice (see Fig. 6) acting as an almost complete reflector, but at strongly inclined incidence, for TM light – and a nearly perfect transmitter for TE light. The authors note that the use of a slightly distorted right-angle T-junction structure, together with incidence at 45°, provides a good approximation to the classic (and, in a historical sense, Scottish) phenomenon of Brewster's angle.

The work of Ao and coworkers [17] provides what can be considered as a significant milestone in the evolution of experimental PhC structures, because (as already mentioned) it provides one of the first reasonably convincing

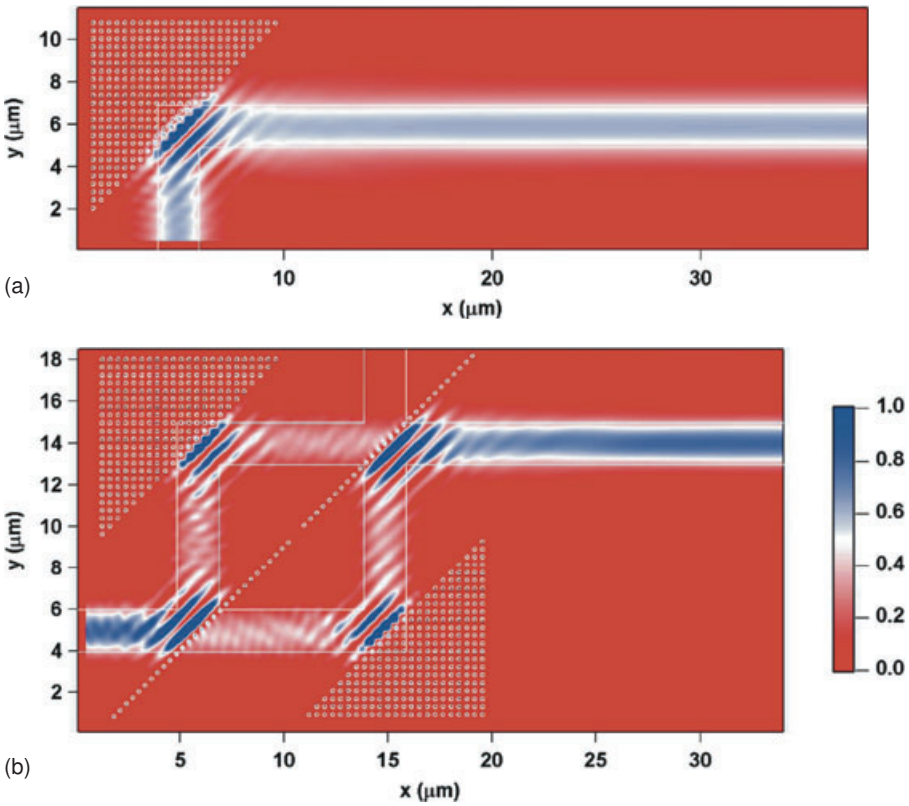

Figure 5 (online color at: www.lpr-journal.org) (a) Simulated interaction of a wide (enough) light beam with a PhC corner reflector [22] – and (b) combination of two PhC corner reflectors and two PhC beamsplitters to form compact Mach–Zehnder interferometer. In this case the beam width was defined by a waveguide that was only 2 μm wide, i. e. approximately four scaled wavelengths.

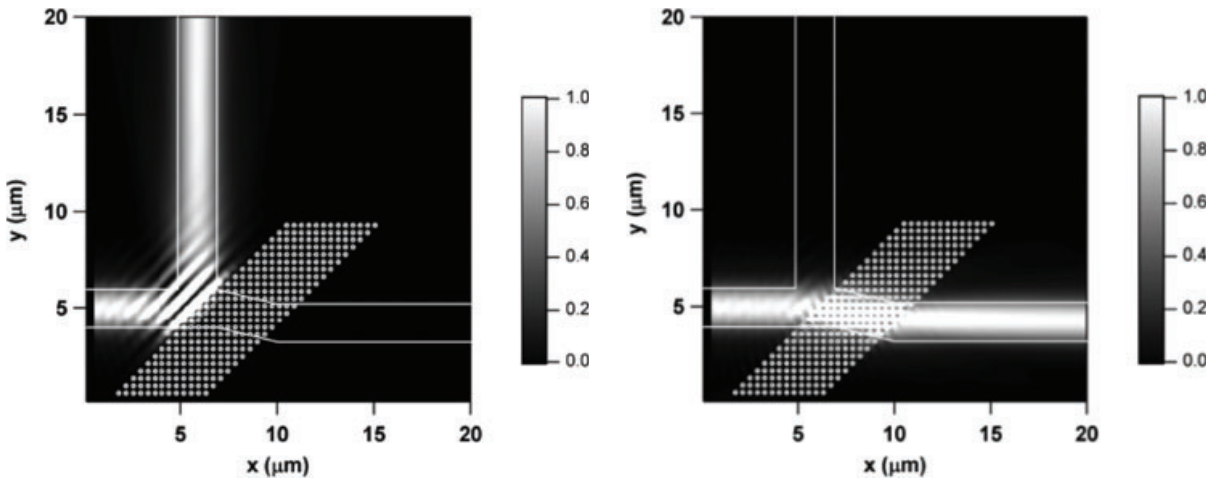

Figure 6 Polarization selective action of pillar-based 2D PhC beamsplitter structure [23].

demonstrations of an actual fabricated *pillar*-type 2D PhC structure with viable practical behavior at optical frequencies. The use of amorphous silicon, which can readily be deposited at micrometer or even greater thicknesses, is an important ingredient in this successful realization. Although there is a substantial level of correspondence between the structure fabricated by Ao et al. [17] and the structures modeled some years earlier by Nordin et al. [22–25], the operating principles are significantly different. In the beamsplitter structure realized by Ao et al., the light arrives in a wide waveguide – at normal incidence – on a region of 2D PhC having a triangular (hexagonal) lattice symmetry. After entering the PhC region, the incident light propagates along two entirely different directions that are determined by polarization. Figure 7a shows a scanning electron micrograph of the actual device structure, while Fig. 7b shows the simulated propagation through the structure, taking account of the polarization-selective behavior.

The extent of the polarization discrimination provided by this PhC beamsplitter/waveguide combination, over a reasonably useful range of wavelengths, is shown in Fig. 8, also from [17]. The plots of transmitted power versus wavelength in Fig. 8a are for output waveguide 1, while the substantially complementary results for output waveguide 2 are shown in

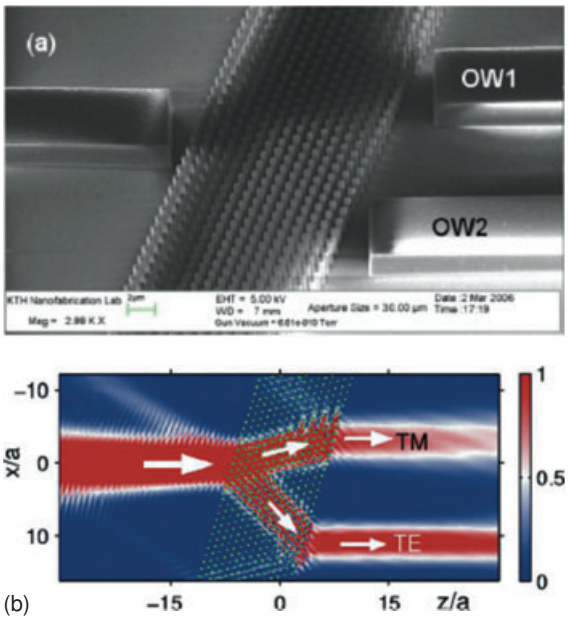

Figure 7 (online color at: www.lpr-journal.org) (a) SEM image of pillar-based PhC beam-splitter fabricated in an amorphous silicon film, in a silicon on-insulator (SOI) waveguide format on a silicon lower cladding layer – reprinted with permission from [17]. Copyright 2006, American Institute of Physics. The input waveguide stripe is on the left-hand side of the image – and the two output waveguide stripes are to the right of the PhC region. (b) Simulation of polarisation dependent propagation through the PhC beam-splitter structure – reprinted with permission from [17]. Copyright 2006, American Institute of Physics.

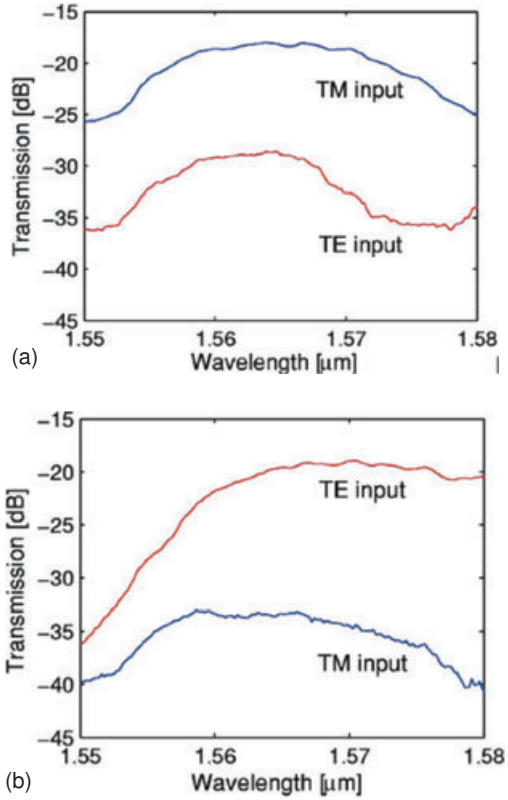

Figure 8 (online color at: www.lpr-journal.org) (a) Transmitted power versus wavelength for pillar-based PhC beamsplitter: waveguide 1. (b) Transmitted power versus wavelength for pillar-based PhC beamsplitter: waveguide 2. Figures reprinted with permission from [17]. Copyright 2006, American Institute of Physics.

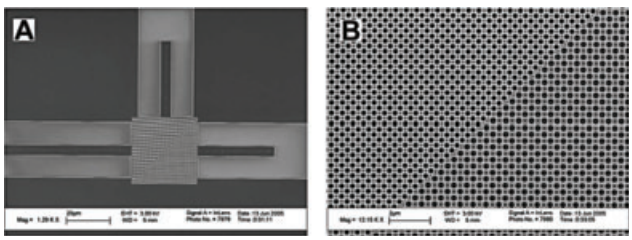

Figure 9 Scanning electron micrographs of a PhC heterostructure beamsplitter at different magnifications, after [26].

Fig. 8b. Although these results show a convincing measure of polarization discrimination for each output waveguide, our view is that the discrimination level obtained is likely to be insufficient for the requirements of a practical application (e. g. in terms of the ratio of the power in one polarization to that in the other polarization). If it is felt that an insertion loss of the order of 20 dB and an orthogonal polarization output power ratio in the range from 10 to 15 dB is not sufficient performance, there is the challenge of realizing a device structure with seriously superior performance. Additionally, the several decibel variation in the transmitted amplitude over a wavelength range of more than 0.01 μm could be problematic in practice. A detailed understanding, informed by modeling, of the contributions of scattering and interface reflection losses, leakage and modal distributions – in all three space dimensions – will be required.

Because of the basic bandgap properties of 2D PhC lattices, light arriving at the straight-line, diagonal, interface between two PhC regions that have the same (square) lattice symmetry – but different lattice periods – can provide usefully polarization-dependent beamsplitting properties. In the case of the paper by Schonbrun and coworkers [26], a 90° beamsplitter was realized via an abrupt interface at 45° between two square PhC lattices with the same filling factor and lattice orientation, but different periodicities. Micrographs of the structure are shown in Fig. 9. Much more general situations – with different lattice symmetries, lattice constants, lattice orientations, filling factors and interface orientations are clearly possible. Such general situations provide a domain in a multidimensional parameter space that it may be interesting to investigate with the aid of some form of optimization algorithm. For operation at wavelengths that are a little longer than 1500 nm, respective lattice constants of 353 nm and 438 nm were used in a single depth mode SOI waveguide with a 300-nm thick core [26]. Because of the detailed nature of the angular dependence of the Bloch mode propagation velocity on direction (and also on wavelength), an important property of the square lattice PhC structure could be incorporated into the device design – self-collimation of the light beam delivered to the beamsplitter interface.

In some ways the most advanced manifestation of a beamsplitter device in the literature is the one that has been described, analyzed and realized by Zabelin and coworkers [27]. This device exploits the polarization dependence of propagation in a 2D periodic PhC lattice of holes that have a suitably chosen diameter and are etched deeply into a vertically weakly confined planar waveguide. This configuration is, therefore not based on the membrane waveguide or the large index contrast silicon-on-silica waveguide that are now commonly used. As is shown in Fig. 10, the beamsplitting 2D lattice gives a 90° rotation in propagation direction for most of the TE light arriving on it at a 45° angle of incidence. In contrast, TM-polarized light largely propagates straight through the beamsplitter structure without deviation.

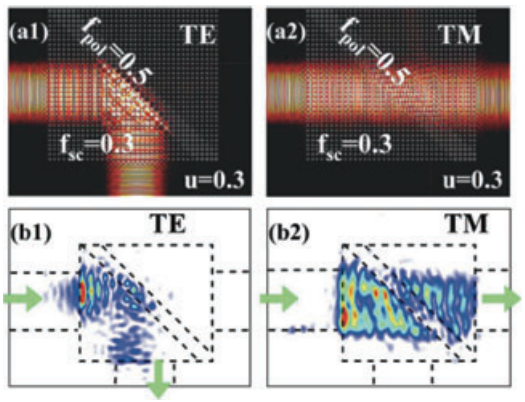

Figure 10 (online color at: www.lpr-journal.org) Simulated propagation through the 2D (square lattice) for the two different basic polarizations, from Zabelin et al. [27].

Other work on an alternative PhC beamsplitter concept has been described by Wu et al. [28]. In that case, the beamsplitting action demonstrated was the strongly wavelength dependent angular dispersion, of the selected quasi-TE-polarized light, that is characteristic of a superprism. The device configuration was such that a light beam entering the superprism region along a single, fairly wide, stripe waveguide could be directed, according to its wavelength, to one of several output waveguides. Prather and coworkers [29,30] have demonstrated, both in simulation and experimentally, a version of a corner reflector bend and also beamsplitting action in 'bulk' 2D PhC regions, as well as self-collimation in a bulk 3D PhC structure.

It is the intention of the present article to address the question of practical applicability. So we propose the basic question: 'what are beamsplitters for?' But perhaps a more appropriate question is: 'what situations in a waveguide-based planar photonics environment intrinsically call for beamsplitters that are based on photonic crystal principles?' Our view is that, with the defining principles that we have applied in reviewing the existing body of research literature, beamsplitting devices could be a useful ingredient in an integrated optics technology in which stripe waveguides that are at least several free-space wavelengths wide and where the lateral (i. e. inplane) contrast in the *effective* guided mode refractive index is small. If the wide-stripe waveguide is laterally single moded, propagation is only approximately plane wave – and device design should take account of this fact. Passage from a simple, but wide, stripe waveguide into a photonic crystal region that can both perform beam-collimation and beamsplitting functionality provides a conceptually desirable route to good device performance. But obtaining truly well-engineered beamsplitter devices remains a substantial challenge, mostly in terms of the quality of device fabrication – but also in terms of detailed design.

Achievement of sufficiently complete polarization discrimination, where polarization-dependent beamsplitting is a requirement, remains a major challenge for the level of device fabrication technology currently available. Likewise, achieving a polarization-independent value of the power-splitting ratio that is nearly constant over a large enough range of wavelengths remains a design and fabrication challenge.

Detailed comparison between the performances demonstrated in the various different forms of PhC-based waveguide beamsplitter that have been described above is arguably premature – with only 'proof-of-principle' performance levels being achieved.

Historically, the use of the word *beamsplitter* for a specific type of optical waveguide device goes back at least as far as the work of Pennington and Kuhn [33] more than forty years ago, while a somewhat more recent paper [34] described much the same device configuration but failed to use the word beamsplitter in its title. Literature searching based on the keyword combination 'optical waveguide beamsplitter' reveals a quite diverse range of device formats, e. g. the paper by Ovchinnikov [35]. This diversity extends to the various specifically photonic crystal devices that we have considered above. A further point is that there is no single configuration that can unarguably be described as a standard one – and it is not even certain that any of the optical waveguide beamsplitter devices described in the research literature have successfully migrated to routine use in integrated optical subsystems. Our view is that beamsplitters based on photonic crystal principles, taken in a broad sense, could be developed to a commercially useful performance level, provided that a substantial amount of well-directed technological and design work were carried out.

7. Slow light and backward-wave propagation

This section begins with an immediate qualification that is necessary in order to give an appropriate historical perspective on the nature of light. This perspective is routinely overlooked by many of the people who form what may be called 'the slow-light community'. This qualification is of a fundamental nature that goes back at least as far as that celebrated Scot, James Clerk Maxwell. The vital point is that, apart from their frequency, there is no intrinsic distinction between radio waves and optical waves. Both are electromagnetic waves that are generated and propagate according to the predictions of Maxwell's equations [36]. Of course, quantum phenomena that justify the use of the

language of photon processes (generation, annihilation, photon splitting via spontaneous parametric downconversion, etc.) are unavoidable aspects of the physics of light – while they do not impinge to anything like the same extent at radio frequencies.

The generation and exploitation of slow electromagnetic waves, with specifically *microwave* connotations, goes back to the second world war (to the year 1943) and to Rudi Kompfner in particular [37]. It was Kompfner (a professional architect!) who first discovered (or rather invented) the possibility of making electromagnetic waves travel more slowly by forming a helical coil of metallic wire and launching waves at a microwave frequency onto that spiral. A schematic diagram of the device, called the travelling wave amplifier (TWA) taken from Kompfner [38], is shown in Fig. 11.

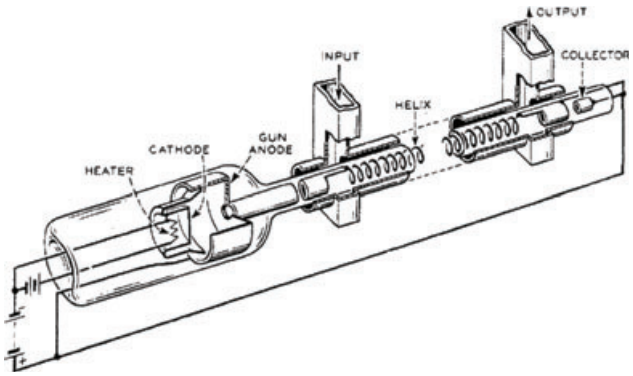

Figure 11 Schematic diagram of the construction of a TWA – from Kompfner [38]. The operative parts of the device include the heated cathode, which emits electrons that are then accelerated, by a large positive voltage, through the anode. Waveguide-confined electromagnetic waves are coupled onto the helical travelling wave electrode structure – and coupled out after amplification through the interaction of the electromagnetic travelling waves and space-charge waves in the electron beam.

Electrons are emitted from the cathode of the device with a spread of velocities, but are then accelerated by a large voltage to a high velocity that may even approach that of light. An electromagnetic propagation velocity reduction factor of $d/2\pi a$ along the axis of the helix, due simply to the geometry of the spiral having a repeat distance of d and circular cross-sectional radius a, was shown to apply. By slowing the electromagnetic wave by a factor of, for example, 10 with respect to the free-space velocity, c, the wave velocity along the axis could be readily made the same as that of electrons emitted by a circular electron gun and accelerated to an energy of only 2.5 k(e)V along the axis of the spiral electrode. The interaction of oscillations on the electron beam with the slow waves that can propagate on the helical electrode structure is the core physical process of the travelling wave amplifier (TWA) [39]. We immediately add here that the electromagnetic wave travelling on a helical electrode structure is intrinsically a Bloch–Brillouin mode, because of the periodicity of the spiral along the defining axis of the cylinder. We also note that the periodic structure used in a TWA is not necessarily a spiral electrode – and that periodically spaced cavities of a similar nature to those used in another microwave frequency electron tube, the klystron [40], are also useful as a travelling-wave amplification structure. A vital practical point is that the electron beam is typically kept together (i. e. confined against Coulombic repulsion forces) by the addition of a cylindrical magnet arrangement.

Since electromagnetic wave propagation may be described in terms of two characteristic velocities, the phase velocity and the group velocity, a natural question is: 'which velocity is the relevant one in the present case?'. The answer is that both velocities are relevant. Propagation along a spiral electrode is dispersive, with the axial phase velocity being characteristically less than that of waves in free space at the same frequency. The group velocity may be close to the phase velocity at low enough frequencies and, in the present case, to the free-space velocity – but, since it is directly given by the local slope of the curve of frequency against propagation constant, the group velocity is typically smaller than the phase velocity. The efficient transfer of power/energy between a high-velocity electron beam and a surrounding structure that supports electromagnetic wave propagation requires that the phase velocity of the electromagnetic wave be matched closely with the electron velocity. While electrons moving through a vacuum must still be subject to *wave–particle duality* – which does imply a characteristic wavelength directly related to the electron momentum – the important point in the present context is that there is a specific form of plasma oscillation in a beam that consists purely of negatively charged particles. This oscillation is a '*space-charge wave*' and takes the form of some electrons travelling locally at slightly more than the average velocity of the beam and some electrons travelling locally at slightly less than the average beam velocity. Analysis of space-charge waves in electron beams goes back to the seminal paper of S. Ramo (one of the founders of the TRW company) in 1939 [41]. We make the further point that the phase velocity of a Bloch mode in a periodic medium is not a unique number, because of the cyclic nature of the Bloch harmonics. But in the travelling wave amplifier (TWA), the relevant phase velocity is determined by the $\omega - \mathbf{k}$ coordinates of a point on the dispersion curve(s) that lies in the first Brillouin zone, where the slope, and therefore the group velocity, is also positive.

But what about the backward wave oscillator (BWO)? The fundamental point about the helical travelling-wave electrode structure is that it is periodic along the defining axis of the spiral, with the result that the modes of electromagnetic propagation are Bloch modes with a characteristic space-harmonic spectrum. Coupling between electrons moving with a well-defined velocity along the axis of the travelling wave electrode structure and the electromagnetic Bloch modes of the spiral electrode structure can cause energy transfer to the electromagnetic wave, leading to amplification. But Bloch modes in periodic structures can have opposite group and phase velocity, so that the direction of the growing electromagnetic wave can be opposite to that of the direction of motion of the electron beam –

and the device can then become an oscillator: a backward-wave oscillator [42, 43]. The BWO operates on the classic electronic oscillator model of an amplifying system with positive (more generally, phase-controlled) feedback and the build-up to a coherent oscillation arising from the action of frequency selectivity on noise fluctuations in the electron beam. BWOs are commercially available sources of coherent electromagnetic waves, with some examples capable of generating frequencies as high as 700 GHz.

One justification for our mentioning the TWA and BWO here is that recent research by Zheludev and coworkers [44, 45] has demonstrated that a suitable periodically alternating metal–dielectric stack through which moderately high energy electrons are launched, via a few hundred nanometer-size hole, can generate *light* at visible wavelengths. The authors of these papers cite as antecedent the historic paper of Smith and Purcell [46], which demonstrated that light could be generated by irradiation of a metallic diffraction grating with a 300-kV electron beam, in grazing incidence – but make no reference to the possibly close analogy of their experiments with the mode of operation of the microwave frequency sources that we have just cited. Simple calculations of the relationship between acceleration voltage and electron velocity suggest to us that space-charge waves in the electron beam, at the voltages in the range 20 to 40 kV used by Zheludev and coworkers, can have approximately the same velocity as the Bloch modes of the structure formed by the nanohole drilled through a metallo-dielectric stack having 11 layers with a periodic repeat distance of 200 nm – leading to light generation at the observed wavelength around 750 to 900 nm. This close (enough) matching situation suggests the possibility that space-charge waves in the electron beam produce the light generation from the nanohole. Because the hole is 'blind', i. e. terminates in solid material, the electron motion could well be locally much more complex – and the mode of operation could be essentially a combination of BWO-like behavior and reflex-klystron-like behavior.

However, the excellent review paper by Gover and Yariv [47] sets out clearly an important basic aspect of the interaction between an electron beam and a periodic electromagnetic wave propagation supporting structure. Two distinct regimes can be identified. With sufficient current density and confinement, the oscillation of the electron-beam takes the form of space-charge waves – in which the repulsion forces between electrons in the electron cloud play an important role. This situation is typical of the TWA and BWO. At low enough levels of current density and confinement, the repulsion forces between the electrons are weak and the interaction can be regarded as having a 'single-electron' character. The latter case applies typically to the Smith–Purcell experiment and its descendants. Detailed analysis, based on an accurate characterization of the experimental situation, should make it possible to distinguish between regimes or identify a possibly intermediate situation. The results of the analysis could then be useful in designing devices for optimum performance.

We now turn to the topic of slow-light propagation in structures that specifically fit with the label photonic crystal (PhC). A recent review article by Talneau [48] covers this topic at a useful level – and highlights some of the critical issues for photonic crystal devices in which slow propagation is a central aspect of device operation. While reduction of the group velocity to as little as $c/100$ may be experimentally feasible, with its beneficial implications for very compact delay structures, reality strikes hard in terms of severe irregularity in the spectral response of devices actually realized. Even with the acceptance of much smaller slowing factors, S, like 4 (corresponding to a group velocity of approximately $c/14$), there are serious problems of an engineering nature, because of the need not only to reduce the group velocity – but also to eliminate group-velocity dispersion (GVD), as well as reducing higher-order dispersion terms.

The slowing factor, S, is defined as the proportional amount by which the velocity of propagation of light (or, more generally, electromagnetic waves) is reduced with respect to that of light in the primary bulk medium in which the photonic crystal structure is embedded. In silicon, $S = 1$ is equivalent to a group refractive index of approximately 3.5. Only through deliberate dispersion engineering can seriously useful time–bandwidth delay products possibly be obtained in real devices. The end result of design for good dispersion management is that information transmission in the form of high repetition rate trains of short pulses becomes possible in a single compact delay-line device – over a usefully wide wavelength spectrum. But another measure of delay-line performance involves assessment of how many bits, at a high data rate, might be stored in a delay line – and whether it is possible to store, for example, a whole 8-bit byte.

A substantial body of literature now exists on slow-light propagation in PhC channel guides. A notable contribution to the development of the slow-light approach in PhC channel waveguides came with the publication of the work by Frandsen and coworkers [49], following earlier modeling work by Petrov and Eich [50]. In this work, the vitally important ingredient is understanding that it is possible to modify a 2D photonic crystal channel waveguide so that not only is group-velocity dispersion (GVD) zero at a particular specified frequency, but also that higher-order dispersion terms can be modified – and greatly reduced. The end result of the research that has now been carried out in this domain by several groups is that it has become possible to design PhC channel waveguide structures that can provide compact propagation delay functionality over a usefully wide range of wavelengths [51, 52].

The approach of Frandsen and coworkers [49] started conceptually with a W1 PhC waveguide formed by 'removing' a line of holes along the ΓK-direction of a block of hexagonal lattice PhC, followed by reducing the diameter of all the holes in the rows immediately adjacent to and on either side of the channel by a designed amount – and *increasing* the diameter of all the holes in the adjacent rows, also by a (different) designed amount. See the scanning electron micrograph in Fig. 12.

The nomenclature 'W1' simply describes the optical *waveguide* formed in a 2D region of photonic crystal lattice

Figure 12 (online color at: www.lpr-journal.org) Micrograph of W1 PhC waveguide with modified hole diameters in four rows of holes (two on each side of the waveguide channel), reproduced from [49].

when *one row* of holes is filled in, without displacing the rest of the 2D lattice in any way. The realization of a slow-light structure, such as that shown in Fig. 12, illustrates an important point that applies more generally in PhC devices. The point is that it is necessary both to introduce a basic modification of the regular PhC lattice (in this case, by removing the holes to form the W1 waveguide) and then carry out an additional modification process. In the present case, the additional modification consists of changing the diameters in selected rows of holes. In other situations, both hole positions and diameters may usefully be changed. An example of this last approach was its successful application to improving the transmission of light through abrupt bends [53]. A quite distinct approach to PhC channel waveguide design for dispersion-managed slow-light purposes has been designed computationally around the use of PhC lattices with holes that have a controlled amount of ellipticity [14, 51].

Krauss [52] has examined the question: 'Why do we need slow light?' – and highlighted strong light–matter interaction, enhanced nonlinearity (with particular mention of Raman amplification), quantum photonic behavior, optical information/data storage and delay as some of the motivations for attempting to exploit slow light in photonic crystal based devices. Arguably, slow light is most desirably exploited in PhC devices that supply the switching and modulation functions.

7.1. Switches and modulators in slow-light PhCs

The possible exploitation of photonic crystal structuring in devices that perform switching or modulation functionality connects quite naturally with slow light. Once it has been recognized that the strength of the electro-optic effect, for example, effectively increases in proportion to the slowing factor, S, it becomes fairly obvious that slow-light behavior can be exploited to produce more compact devices for switching and modulation. For the present purposes, the word 'electro-optic' should be understood to mean, in the first place, the linear (Pockels) electro-optic effect. But a number of other effects can possibly be exploited, starting with the quadratic (Kerr) electro-optic effect. Because of its quadratic characteristics, the Kerr effect will increase with the slowing factor as S^2– an attractive feature, since the Kerr effect occurs in all media, while the Pockels effect requires noncentrosymmetric single-crystalline or oriented polycrystalline material.

Comparisons may be made between slow-light and 'fast-light' devices in terms of either device size (i. e. the interaction length in an electro-optic or thermo-optic device) or operating voltage/power. We make here a comparison between the slow-light PhC directional coupler thermo-optic switch of Beggs et al. [54] and the optically biased Mach–Zehnder thermo-optic modulator structure of Camargo et al. [55, 56]. The latter device, for the wide-bandwidth (in terms of wavelength spectrum) operation selected, is undoubtedly *not* in the slow-light regime. Both devices are compact, with a core length of only 5 μm in the former and a somewhat greater length of 12 μm in the latter. Remarkably, the power requirement (28 mW) in the latter (fast-light) case is considerably smaller than in the former (slow-light) case (168 mW).

But this difference in operating power requirement by an amount that approaches an order of magnitude (in the wrong direction!) is primarily a manifestation of the better (in a nonjudgemental sense) thermo-optic design and construction of the M–Z PhC device of Camargo et al. [55]. This apparently contradictory result does not negate the more fundamental point that an order of magnitude smaller index change (6.8×10^{-3} c. f. 6.45×10^{-2}) was required for operation in the more than two times shorter slow-light device [54]. This result does, however, also make the point that the full benefits of exploiting slow-light behavior are only accessible in a convincing manner when all aspects of device design and construction are addressed.

The channel waveguide PhC modulator and directional coupler structures of Refs. [54–57] were not deliberately targeted at slow-light behavior, but were nevertheless very compact and readily controllable thermo-optically. The PhC waveguide directional-coupler configuration is a natural choice as a vehicle for slow-light-based optical switching functionality [54] – and the quality of the switching transfer characteristics obtained is impressive, while the on-off ratio quoted would still be a serious limitation for a practical system. An important conceptual contrast can be made with the classical directional-coupler, integrated-optical switch – which relies on modifying the interference between the symmetric and antisymmetric *supermodes* of the directional coupler via induced changes in the propagation velocity of *both* supermodes. The concept of supermodes is applicable in arrays of coupled optical waveguides that involve two or more individual waveguides. A supermode is an eigenmode of the coupled system. In the simplest case of identical waveguides that are identically spaced, there will be a number of supermodes, with distinct field and power distributions that is equal to the number of waveguides constituting the array. For the two-waveguide, directional-coupler, structure, there is a close analogy with the two characteristic modes of a system of two simple pendula coupled by a weak spring.

More generally, the concept of the supermode remains applicable even when the waveguides involved and the coupling between them are not all the same.

In the slow-light situation, the equivalent symmetric and antisymmetric supermodes undergo very different amounts of change in velocity – and the situation is dominated by the thermo-optically or electro-optically induced variations in the velocity of the slow (typically the symmetric) supermode [49].

Krauss [52] makes the judgement that the demonstrable information storage and delay capabilities of PhC-based slow-light structures are likely to remain modest, because of propagation losses and random scattering. We add the possibly more crucial point that the impact of imperfection on propagation in slow-light PhC structures may well manifest itself as *dramatic* fluctuations in the propagation delay and transmission magnitude, as the slowing factor S increases. The consequences of this fluctuation in the delay are well illustrated in Fig. 13, taken from the comparison review paper of Melloni et al. [58].

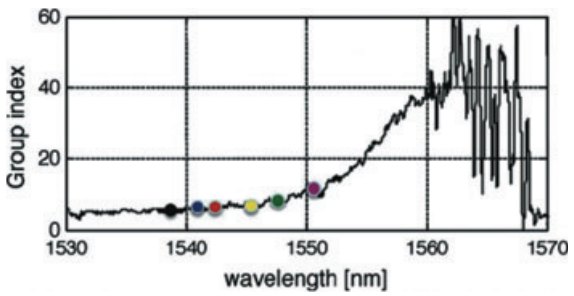

Figure 13 (online color at: www.lpr-journal.org) Experimental variation of group index with wavelength for a PhC channel waveguide – reprinted with permission from [58]. Copyright 2010, IEEE. The circular dots denote points at which observations were made of the associated spectral spread of short pulses of light.

While, as the wavelength is tuned, slow PhC waveguides clearly are able to achieve a target group index of 40, corresponding to a slowing factor, S, greater than 10, the fluctuations in group velocity, for the given structure, at longer wavelengths and higher possible group velocities overwhelm the response. Even where the group index is smaller than 40, the fluctuations are potentially significant – and the impact not only of the random deviation of the waveguide itself, but also the Fabry–Perot oscillation contributions from all of the interfaces and transitions. These considerations suggest that slowing factors below 5 will be obligatory until significant improvements in all aspects of the device realization can be achieved. The very large fluctuations in the group velocity observed at the longest wavelengths in Fig. 13 are presumably a manifestation of strong localization and antilocalization behavior, i. e. versions of Anderson localization. These fluctuations in group velocity have corresponding fluctuations in the transmission spectrum, as is shown in Fig. 5a of [58].

Comparison between the slow-light PhC channel waveguide and the alternative of a photonic-wire ring-based CROW (both types of structure being realized in essentially the same SOI waveguide material) may appear favorable towards the latter, at modest S values. But ring-based CROWs typically have a substantially smaller optical bandwidth – so the standard system basis of comparison, the delay–bandwidth product, provides a more appropriate measure for comparison. The way in which the data being delayed is coded will also, presumably, determine the relative importance of group velocity and its consequent group-delay fluctuation. Another potentially important detrimental factor that applies in the specific case of photonic wire ring-resonator-based structures is coherent backscattering [59].

Localized or global tuning of a PhC slow-light device via mechanisms such as the thermo-optic effect or various 'electro-optic' effects could adjust both the absolute amount of delay and its spectral response – including shifting pass-band edges so that propagation of the light is effectively turned off in selected parts of the spectrum. One early demonstration of the integration of thermo-optic control into a planar photonic crystal device was provided by Chong and De La Rue [60]. The PhC structure used was a moderate quality factor microcavity, directly embedded in a PhC channel waveguide. Thermo-optic tuning was subsequently used by Vlasov et al. [61] in a Mach–Zehnder interferometer arrangement to demonstrate, in a very convincing manner, the possibilities of *controlled* slow-light propagation in PhC waveguides. This device was realized in a suspended silicon membrane and used W1 channel waveguides – but only for a limited part of the propagation path. For this particular structure, the slow-light behavior unavoidably occurred only in the band-edge region of the transmission spectrum

Our view, in accord with that of Krauss [52], is that simple delay – whether tunable or not – is *not* the most promising application for slow light. For example, exploitation of slow propagation in PhC channel guides to provide very compact, low operating voltage, 'electro-optic' or all-optical modulators and switches appears to be more promising. The electro-optic/all-optical effects available for exploitation include the linear (Pockels) effect and the quadratic (Kerr) effect, which may be considered as 'instantaneous' down to less than 10 fs – and other effects, such as the Franz–Keldysh effect and quantum-confined Stark effect (QCSE) in quantum-well-based III-V semiconductor heterostructures. In semiconductors such as silicon and GaAs, injected carriers can provide a potentially useful source of (complex) refractive-index change at modulation/switching rates that are relevant for optical communications purposes.

Electro-optic devices based on slow-light propagation in silicon PhC channel waveguide structures have been demonstrated, for instance by Brosi and coworkers [62] and by Wülbern and coworkers [63]. Adding an electro-optic polymer into strategic locations in silicon PhC waveguide switch structures allows exploitation of a powerful combination of strong confinement, slow propagation, modal electric-field enhancement and the potentially greater electro-optic coefficients of the polymer. The modal electric-field enhancement is due to the continuity of the electric flux density component normal to the interface between a medium with a high dielectric constant and one with a low dielectric constant.

7.2. Nonlinearity and slow light in PhC structures

In pioneering work on the impact of slow light effects on nonlinear behavior, Baron and coworkers [64] found that two-photon absorption (TPA) is arguably more important in slow-light PhC waveguides fabricated in GaAs than for structures fabricated in silicon, since the TPA coefficient for GaAs in the relevant wavelength range is substantially larger than that of silicon. The larger TPA coefficient implies that the nonlinear behavior of slow-light devices realized in GaAs is, at the fiber-optical communications wavelengths with which we are most typically concerned, dominated by the much larger refractive-index change produced by TPA in GaAs than in silicon, as well as the larger amount of absorption in GaAs.

Ikeda and Fainman [65], in an important paper that deserves to be more widely read and understood, show that the nonlinear, Kerr-effect based, figure-of-merit (FOM) in materials relevant to our present study, at wavelengths close to 1.55 μm, is substantially larger for silicon than for GaAs. The FOM takes account both of the n_2 nonlinear coefficient of the material (which is three times larger for GaAs than for silicon) and the attenuation – which is much larger in GaAs, because of its much greater (by more than 10 times [65]) TPA coefficient. The end result is that the FOM for GaAs is about three times smaller than that of silicon. A further comparison – and one that is vitally important for practical all-optical devices – should also be made when the core of the waveguide in which the slow-light PhC structure is realized is the epitaxially grown ternary compound $Al_xGa_{1-x}As$, with progressively greater x-fraction. The greater the value of x, the greater is the direct electronic bandgap of the material, while the n_2 coefficient progressively (but slowly) declines. At $x = 18\%$, the nonlinear FOM is already one order of magnitude greater for $Al_xGa_{1-x}As$ than for silicon, while at $x = 36\%$, the FOM has increased by a further order of magnitude. The slow-light structure of Inoue et al. [66] was based on material with $x = 26\%$ – and calculation indicates a FOM that is something like 40 times *greater* than that of silicon – and therefore, at least, comparably as large as for any practical alternative material system.

Rawal et al. [14] have shown that, at comparable power density levels and slowing factor values, silicon-based PhC slow-light waveguides can be realized as effectively in relatively thick silicon waveguide cores supported by a silica cladding, with no cover material – as in unsupported (and therefore inherently fragile) thin silicon membranes. In subsequent work [67], it was shown that the dispersion control that is required for soliton formation and broadband delay enhancement can be obtained simply by moving from PhCs based on circular holes (with several different hole diameters being required in a single structure in the 'engineered' case) to a specific choice of elliptical hole parameters in uniform arrays of elliptical holes. The estimated in-waveguide optical power level required to obtain a decisive wavelength-selective switching effect was 2 W, at a group velocity of $c/99$, while Monat and coworkers [68, 69] experimentally required a peak power level of 45 W at a group velocity of $c/50$. This apparently large superiority for the lower cladding supported elliptical-hole structure will, in practice, be substantially eroded for slow-light propagation in structures with the propagation losses and group-velocity fluctuation values – because, in particular, of random-structure scattering – that have been achieved to date experimentally.

The TPA-dominated result of Fig. 3 in [64] is notable because it requires a peak power level of only 0.5 W, together with a group velocity that has been reduced only to $c/9$. Therefore, where TPA is an acceptable process for the modification of slow-light enhanced propagation, GaAs scores significantly by comparison with silicon. But the acceptability of using TPA becomes much reduced if the pulse repetition rate increases to values above, say, 1 GHz and/or the photoexcited carrier lifetime is sufficiently long, e. g. substantially greater than 1 ns. The almost purely Kerr nature of the nonlinear behavior of sufficiently large-bandgap ternary alloy $Al_xGa_{1-x}As$ [65] suggests that devices realized in this material merit further investigation at substantially reduced group velocities, e. g. in the region of $c/50$. Fabrication quality will probably be a predominant practical consideration.

7.3. Coupling into and out of slow-light structures

The question/issue of coupling of light efficiently into and out of slow-light structures, and, in particular, the coupling of light into and out of photonic crystal channel waveguides operating in the slow-light regime has been recognized as a vitally important one. Pottier and coworkers [70] considered a situation where a photonic-wire-type stripe waveguide could be coupled efficiently with a W0.8 PhC channel waveguide via a geometrically tapered structure – as illustrated in Figs. 14a and b.

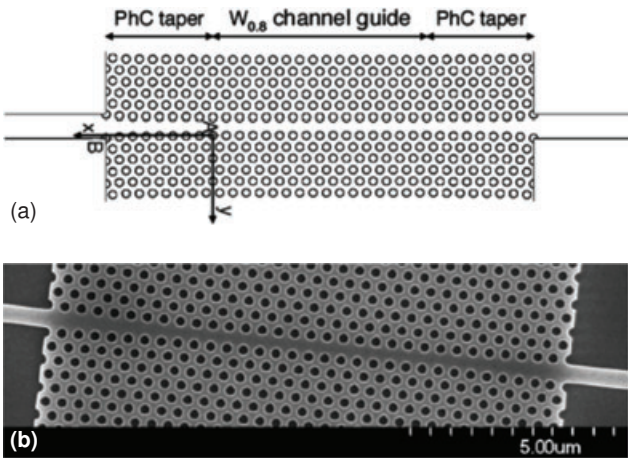

Figure 14 (a) Schematic, to scale, of W0.8 PhC channel waveguide – coupled, via tapers, to external stripe waveguides. (b) SEM image of the same structure. Images extracted, with permission, from [70].

It may be noted that Petrov and Eich [50] had previously shown that a W0.7 PhC channel guide could be (re-)designed so as to have both 'near-zero' group velocity ($0.02c$) and minimal group-velocity dispersion (GVD). 2D

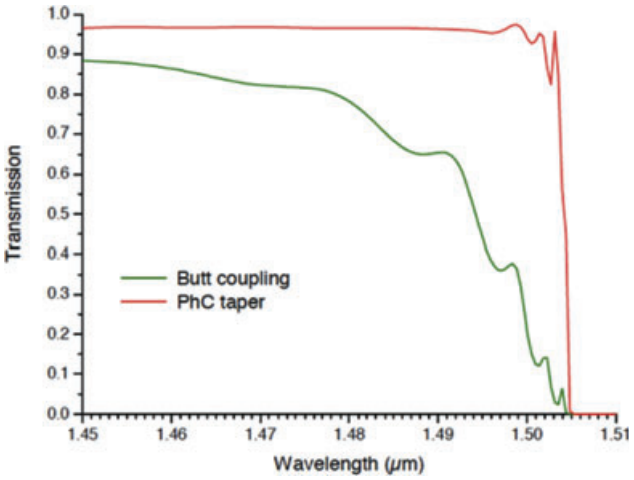

Figure 15 (online color at: www.lpr-journal.org) Transmission through a W0.8 PhC channel waveguide. The green curve is for a simple butt-coupled situation, while the red curve is for a situation with tapered transition regions, as shown in the previous figure [70].

simulation, using an effective index model for the silicon waveguide properties, showed the potential for obtaining a large improvement in the transmission – as shown in Fig. 15.

Affection for the particular version of a transition to slow-light PhC waveguides shown in Fig. 14 was, even if it existed at all, short-lived. Earlier work by the same authors (see Fig. 5 of [71]) had produced an arguably more interesting phenomenon – a demonstration of an early version of the so-called 'trapped rainbow' effect identified more recently by Hess and coworkers [72, 73], i. e. essentially an optical frequency version of the kind of frequency/wavelength dependent position of the propagation cutoff observed many years earlier in a tapered hollow metal waveguide at microwave frequencies [74].

The modern era of transition structures for going to and from the slow-light channel waveguides – with close to 100% transmission, large bandwidth and very short transition distances, even for very large differences in the velocity – was heralded by the conceptual paper of Velha and coworkers [75]. Shortly thereafter, there followed the paper by Hugonin and coworkers [76] that was specifically targeted on the PhC channel waveguide taper. Subsequently, White and coworkers [77] have demonstrated optimized structures with transition zones that could, in principle, shrink to a length of zero.

8. Microcavity resonators

Microcavity resonators based on both 1D periodic and 2D periodic PhC configurations arguably form the most important success story in the photonic crystal saga. An important early milestone in this domain was the 1D PhC microcavity described by Foresi and coworkers [78]. This paper was notable for achieving what seemed at the time like a respectably high resonance quality factor (Q-factor) of 265 – and also for using a lower cladding-supported photonic-wire waveguide in SOI – together with two closely space mirrors consisting of four periodically arranged holes, 'embedded' in the wire waveguide. This structure was, in substantial measure, a version of a Fabry–Perot cavity, with the transmission resonance being spectrally located within a wide stop-band. Interestingly, the paper by Foresi and coworkers [78] was preceded by two papers concerned with a similar type of 1D PhC mirror cavity structure, but with an air-bridge configuration [79, 80]. The potentially very high Q-factor of this microcavity configuration was clearly identified in the purely theoretical paper by Chen and coworkers [79], while actual air-bridge structures fabricated in both SOI and III-V semiconductor material systems were demonstrated by Villeneuve and coworkers [80], but without any experimental results. The dimensions of the features in the structure clearly suggest that the target wavelength was well into the mid-infrared. Somewhat later, valid experimental results were obtained, at fiber-optical communications wavelengths, for both 'monorail' (i. e. high aspect-ratio) and air-bridge (i. e. suspended) waveguide geometry cavities with pairs of simple periodic four-hole mirrors embedded in them [81]. A significant point is that the material system used, in this case, was the $Al_xGa_{1-x}As$/GaAs system, with x being large enough (93%) to give strongly selective oxidation of the relatively thick $Al_xGa_{1-x}As$ lower cladding layer. Leaving this oxidized layer in place provided a high refractive index contrast ($n = 1.6$) lower cladding layer for the monorail waveguide geometry – while localized wet etching was used for selective removal of the oxidized layer to form the air-bridge microcavities. In all this experimental success, the highest Q-factor value obtained was only 260, providing a strong contrast with the earlier computed predictions of Q-factor values of several tens of thousand for a nominally identical air-bridge microcavity [79]. This discrepancy is not an intrinsically insuperable one – and primarily reflects the difference between a valid computational design and the structure that was actually fabricated.

There was then a gap of several years before the appearance of the papers by Jugessur and coworkers [82, 83], which used a well-supported narrow-ridge waveguide realized in an $Al_xGa_{1-x}As$ epitaxial waveguide, again with 1D periodic mirrors. This work was notable, despite the modest Q-factor values obtained with the deep hole, *low* vertical index-contrast approach – because of its use of tapered hole-size arrangements on the input and output sides of the cavity, together with periodic mirrors, in an attempt to increase the overall transmission of the cavity. The earlier paper of Krauss et al. [84] had also used the deep-etching approach in a low vertical index-contrast waveguide ridge, but with the 1D periodic mirrors being formed by slots across the whole width of the waveguide.

The same 'full-width', deeply etched mirror approach was successfully applied in realizing short cavity, low threshold-current microcavity lasers. Krauss and coworkers [85–87] demonstrated the operation of electrically pumped semiconductor diode lasers with cavity lengths as short as 20 μm and 1D periodic mirrors across waveguide stripes that were as much as 8 μm wide. The lowest

threshold current, below 6 mA, was obtained with a cavity length of 40 µm. Happ and coworkers [88] obtained somewhat superior performance, in terms of nominal current density, with much longer (cavity length of 600 µm) lasers having ridge-waveguides that were 2 µm wide – by using a combination of a single 2D PhC mirror and a cleaved-facet mirror at the other end of the cavity. Later work by Erwin and coworkers [89] brought the threshold current down to below 2 mA in lasers that used an active junction defined by an oxide aperture of approximately 5 µm width, together with a cavity length of 84 µm. It is of interest to note that somewhat similar grating structures, etched into ridge waveguides but less deeply, were used to investigate the possible formation of gap or Bragg solitons – through nonlinear propagation [90–92].

Reverting to the topic of microcavities formed within 2D PhC regions, we observe that, as early as 1998, Smith and coworkers [93–95] successfully demonstrated that moderately high Q-factor ($Q \sim 1000$) microcavities could be realized by removing holes from a hexagonal 2D PhC lattice. In this case, the luminescence required to drive the experiment was derived from photopumped quantum dots embedded in a III-V semiconductor epitaxial waveguide – and the deeply etched hole, low vertical index-contrast approach was used. Subsequently, lateral coupling from a PhC channel waveguide to a 2D PhC microcavity was demonstrated by the same group [95].

A major step forward in the evolution of the photonic-crystal-based microcavity came with the work of the teams of Noda [96–98] and Notomi [99–101]. Two distinct approaches, but with internal variations within each approach, have emerged for producing very high Q-factor values experimentally, although appropriate basic conceptual formulations were required at the start – and these formulations were necessarily accompanied by computational simulation and optimization processes [96].

In the isolated microcavity design of Noda and coworkers, shown schematically in Fig. 16, the cavity is sufficiently long: being formed by a three lattice spacings long region that has three holes removed (i. e. filled in), together with the two penetration depths into the mirrors that are formed in the 2D PhC lattice at either end of the cavity. This structure was realized in a silicon membrane waveguide with air above and below, giving strong vertical confinement. The small, but equal, displacement by $0.2a$, from their true lattice positions, of the two holes that form the geometrical ends of the cavity is a key aspect of this approach.

The schematic of Fig. 16 shows the modal field distribution for the high Q-factor resonance of the PhC microcavity, but this mode is not the only resonant mode that the microcavity exhibits. The schematic does not show how the resonance is fed, but it was demonstrated that a W1 channel waveguide with a separation of three lattice spacings from the defining cavity region was appropriate – enabling retention of the high resonance Q-factor – together with efficient extraction, at the resonance peak frequency, of a large part of the power that is present in the feeder waveguide.

In the double-heterostructure approach to forming high Q-factor microcavities [97, 100], small modifications are made at two carefully chosen interface positions along a W1 PhC channel waveguide that is realized in a 2D periodic hexagonal (triangular) lattice of holes in a silicon (i. e. high refractive index) membrane waveguide. As the above scanning electron micrograph (Fig. 17) shows, the heterostructure cavity can be formed by creating a short section of the W1 channel waveguide that has slightly larger hole diameters, going from 410 nm to 420 nm – a relative change of only 2.5%.

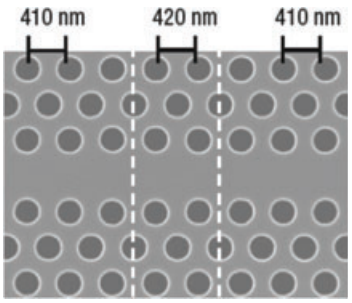

Figure 17 (online color at: www.lpr-journal.org) Annotated scanning electron micrograph of PhC channel-waveguide (double) heterostructure – reprinted with permission from reference [97].

Figure 18 shows the corresponding resonant modal field distribution. Space, time and energy considerations apply to the writing of this article, so we now simply catalog and reference, rapidly, the impressive exploration of the device possibilities that followed on from the demonstration of these two distinct high Q-factor PhC microcavity designs. Device effects that have been demonstrated using such high Q-factor microcavities include nonlinearity, fast switching, light emission and lasing, bi-stability, dy-

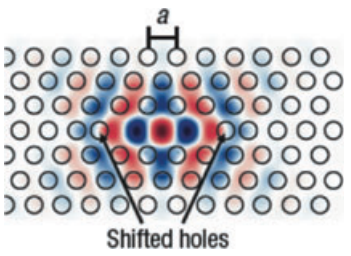

Figure 16 (online color at: www.lpr-journal.org) Sign-dependent plot of the magnetic field component of the high Q-factor mode of the shifted hole microcavity embedded in a 2D PhC region – reprinted with permission from reference [97].

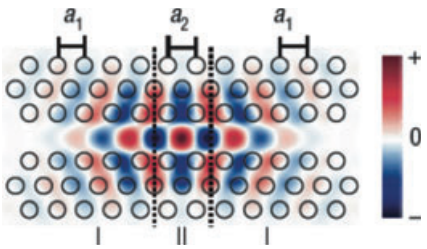

Figure 18 (online color at: www.lpr-journal.org) Schematic of double-heterostructure microcavity formed by varying a parameter of the W1 channel waveguide – reprinted with permission from reference [97]. In this case, the channel width and lattice constant remain unchanged, while the hole radius is slightly increased.

namic control of the cavity Q-factor and switchable light-pulse storage [102–108]. The recent publication by Nomura and coworkers [108] describes the impact of a moderately high Q-factor PhC microcavity ($Q \sim 25\,000$) on the light-emission process from a single Stranski–Krastanow quantum dot of 'indium arsenide' (InAs) embedded in a waveguide membrane of GaAs. Photopumped laser action and significantly modified quantum statistical behavior were observed with this device structure. A later publication by the same authors [109] has produced new insight into the task of obtaining the desired combination of a high Q-factor (as large as 280 000), together with a small volume, $V = 0.23(\lambda/n)^3$ – yielding a very high value of the Purcell factor Q/V.

Periodicity in the optical properties of a structured medium – along a single selected direction – is all that is required for the formation of a stop-band. Deliberate local modification of the periodic structure in any way is sufficient to guarantee that (micro-)cavity behavior will occur. We have already considered structures in which 1D PhC mirror structures have been incorporated into stripe waveguides to form microcavity resonators, compact laser cavities and Bragg/gap soliton forming gratings [79–92]. Subsequent work has seen the evolution of the 1D PhC microcavity towards remarkably high Q-factor values, together with large absolute transmission coefficients on resonance, resulting from the incorporation of various specific deviations from simple periodicity. An important milestone in this approach was the paper by Velha et al. [110], which reported a Q-factor value as large as 8900 that was subsequently improved to 67 000 [111]. Md Zain and coworkers [112–114] made a significant further advance, ultimately achieving an experimentally estimated Q-factor value of 147 000, together with a useful resonant transmission level – and demonstrating a high Q/V ratio (i. e. Purcell factor), because of the very small volume of the resonant mode. The potential for application of such photonic-crystal/photonic-wire (PhC/PhW) microcavity structure in all-optical switching has also been demonstrated [115].

8.1. CROW slow-light structures

The possibility of using slow propagation to provide compact delay via suitably designed channel waveguides through 2D PhC regions has already been considered in some detail in Sect. 7. An alternative approach for obtaining slow light is the use of a series of coupled cavities – an approach that has been implemented with notable success in the case of sequences of coupled ring-resonators formed using stripe-waveguides, aka photonic wire waveguides or photonic nanowires [60, 116–120].

The term coupled-resonator optical waveguide (CROW) was coined by Yariv et al. [121] for an analogous PhC device structure formed by linking individual PhC microcavities, directly in succession. The nature of the transmission versus wavelength characteristics of a sequence of nominally identical coupled resonators depends strongly on the coupling strength between the adjacent resonators. Large resonance quality factor values may be achieved with individual PhC microcavity resonators, implying the possibility, over a narrow spectral bandwidth, of an effective delay distance that is greater, by a multiplicative factor of Q, than the characteristic dimension, its perimeter length, of the cavity. A sequence of N identical weakly coupled cavities can then produce a total delay that is N times the delay for the individual resonator, within approximately the same spectral bandwidth as that of the individual resonators. But this situation is an example of conservation of the time–bandwidth product. Increasing the coupling between adjacent resonators leads to an increase in the bandwidth, at the expense of reduced delay – and greater spectral variation in the transmission amplitude and group delay.

In the case of research on silicon photonic-wire coupled-ring CROWs, the choice, influenced by realistic future systems requirements, has ultimately been to accept quite modest values of the slowing factor, S, around 3 – i. e. equivalent group-velocity values on the order of $c/10$, in order to meet the requirements on bandwidth that come from more advanced, high bit-rate, telecomm systems [116–118]. Work by Jin and coworkers [122] produced PhC CROW structures with a relatively featureless and fairly broad transmission spectrum – but with only nine nominally identical cavities forming the CROW, together with two additional end cavities that were modified by the inclusion of a smaller hole in the middle of these cavities. The design of this particular PhC channel-waveguide-based CROW structure involved fairly weak coupling between adjacent resonators and, probably, modest effective Q-factor values for the individual microcavities forming the CROW. Particular attention was paid to the requirement for a graded transition between the CROW structure and the input and output W1 channel waveguides. As shown in Fig. 19, the graded transition was achieved by retaining the presence of a central, but much smaller, hole in both the first and last cavities of the CROW.

O'Brien et al. [123] have investigated the progressive assembly of CROWs based on heterostructuring of the W1 channel waveguide in a 2D PhC lattice. Choosing to have strong coupling between two nominally identical res-

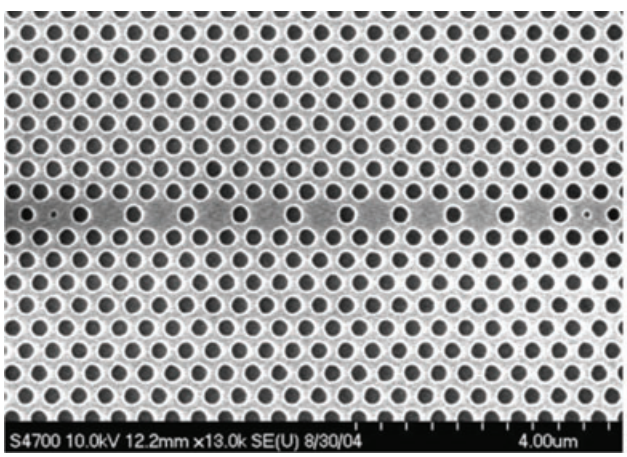

Figure 19 Scanning electron micrograph of CROW structure formed in SOI waveguide [122].

onators produced a distinctly double-peaked experimental frequency response that was reasonably closely matched by theory – for the particular case of the transmission through the two-resonator CROW. This close-match between experimental and theoretical results compares favorably with the two coupled-cavity structures of Jugessur et al. [124] and Md Zain and coworkers [125]. But even for as few as three coupled cavities, the experimental results obtained by O'Brien et al. [123] were considerably degraded – and matched poorly with the theoretical transmission response. For more than three coupled cavities (e. g. ten), a progressively worsening situation was found. Figure 20, taken from [123], shows the regular set of peaks that are generated by computer simulation of a system of 10 identical coupled cavities.

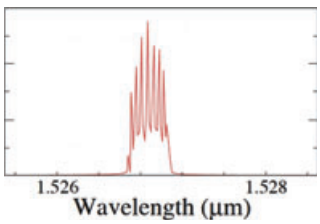

Figure 20 (online color at: www.lpr-journal.org) Simulated transmission spectrum for 10 cavity PhC CROW [123].

Possibly the most extreme versions of the PhC-microcavity-based CROW have been described by Notomi and coworkers [126]. This paper was also the subject of a review commentary by De La Rue [127] – and further commentary by Melloni and Morichetti [128]. Melloni and Morichetti have made a critical comparison of what is possible with the two alternative approaches to CROW structures, i. e. PhC-based and ring-resonator (RR)-based CROWs – from the points of view of data-storage capacity (i. e. buffering), delay tunability, pulse spreading and phase fidelity. This comparison was explicitly dealt with subsequently, in greater detail, in [117]. In broad terms, the conclusion of Melloni and Morichetti was that RR-based CROWs should give superior performance at multiGigabit/s data rates, particularly for more advanced modulation formats, while PhC-based CROWs could win out at Terabit/s data rates.

The irregularity of the spectrum shown in Fig. 21 [126] – e. g. by comparison with the regularity of the computed response shown in Fig. 20 – provides an indication of the scale of the problem, but is actually a substantially superior result

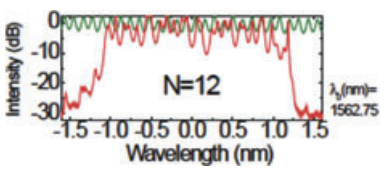

Figure 21 (online color at: www.lpr-journal.org) Transmission intensity spectrum for 12-cavity PhC-based CROW – reprinted with permission from [126]. Copyright 2008, Nature Photonics. In colour in the on-line version: the red trace is the measured transmission spectrum. The green trace shows the transmission spectrum for a single line-defect (W1) channel waveguide with the same parameters.

to the results typically obtained on PhC-based CROWs with larger numbers of sequentially coupled cavities, as described in the same work [126].

9. PhC biosensor structures

One area that has been identified as a target for the application of PhC device structures is the area of biosensing and biomedical sensing [18, 129–131]. The enhancements that apply for slow light and microcavities for other effects, e. g. in the electro-optical and nonlinear optical characteristics, may be exploited to increase the sensitivity of the optical propagation to localized and small changes in the refractive index. For biomedical sensing purposes, one approach that has been exploited uses specific molecular binding such as the antibody–antigen binding process that is characteristic in immunology. By immobilizing a layer of a specific type of antibody on an accessible surface of the PhC waveguide, it is possible unambiguously (in favorable circumstances) to detect the presence of the corresponding antigen in a sample of fluid, e. g. blood diluted in water. Detection occurs through the local refractive-index change that occurs where the antigen is bound, changing the velocity of propagation. In slow-light PhC waveguides, a significant change in the group delay will occur while, in general, the transmission band-edge spectrum of a PhC waveguide will be displaced along the wavelength axis. The very high resonance quality factors (Q-factors) that are possible with photonic crystal microcavities imply that the small perturbation produced by a small number of antigens being bound on to immobilized antibodies can shift the resonance frequency by a readily detectable amount. Arrays of high-Q microcavities, with different resonance frequencies and weakly coupled to feeder waveguides, can be used to identify the possible presence of a 'panel' of several different antigens – and give a profile that can be identified with specific disease conditions [130].

As elsewhere, the PhC-based approach faces stiff competition from the photonic-wire interferometer and RR-based approaches [132, 133].

10. PhC lasers

The history of the PhC laser naturally traces back to the papers by Yablonovitch and Bykov [1, 3]. A key motivation for the invention of the photonic bandgap (PBG) concept, i. e. an omnidirectional stopband in 3-space, was the desire to make a low-threshold laser – ideally with no limit, in principle, to the closeness to zero of the threshold pump level. In the present paper, we shall confine ourselves to consideration of semiconductor lasers realized in heteroepitaxial material that is predominantly formed from III V semiconductor.

One PhC laser format that has been applied successfully uses deeply etched distributed Bragg reflector (DBR) mirrors to form compact cavity lasers. Work using this approach has already been described earlier [19, 20, 85–89] – and is attractive because it avoids some of the issues associated with using membrane structures. The natural configuration

of a vertical diode with its 'back contact' on the lower side of the substrate on which the heterostructure has been grown can be exploited. The issue of nonradiative recombination of hole–electron pairs with an active region embedded in the PhC structure (as in a DFB laser) is largely avoided – by keeping the gain section separate from the PhC structure, which becomes one or more regions of strong and compact DBR mirror.

But an important point for possible photonic integration is that light sources are desirable in which both the contacts of the injection electroluminescent diode are on the top surface. For example, a mesa device geometry or lateral junction diode configuration may be used.

Using the so-called membrane approach brings several key advantages when compared with deep etching of thick laser heterostructures. These advantages include the high spatial confinement of light in very limited volumes, which leads to the possibility of exploiting single-mode planar waveguides, but also of locating accurately the electromagnetic field on a node or an antinode of a layer stack. This configuration makes it possible to significantly enhance or inhibit light emission. These specific properties explain the success of this approach in building high spontaneous emission factor structures and, for example, low threshold microlasers.

The seminal papers on PhC microlasers appeared in the late 1990s and early 2000s. Painter and coworkers [134] demonstrated the first PhC optically pumped microlaser, based on a local defect in a triangular symmetry PhC structure with holes drilled in an InP-based membrane (see Fig. 22). Figure 22 shows both a schematic diagram and a plan-view micrograph of a wafer-bonded heteroepitaxial membrane PhC microcavity-based laser, driven by optical pumping with another (more powerful) laser. The data points show the output light versus pump light (L–L) characteristics, with good evidence of a distinct threshold pump level. Since then, various proposals have been made in order to increase the efficiency, to decrease the laser threshold and to increase the operating temperature of these attractive components.

An important upgrade of the characteristics of these structures was achieved by selecting a configuration more appropriate to mechanical stability and heat sinking than a suspended membrane [135]. Combining epitaxial growth of InP-based semiconductors and molecular bonding on a SiO_2-on-silicon wafer made it possible to reach this goal, thereby opening the way to the integration of III-V-based nanophotonic devices with silicon waveguides, and ultimately with CMOS devices. Such bonded membranes can be considered as generic templates to realize active ultracompact devices such as low-threshold microlasers, integrated on silicon. More recently, alternative approaches based on BCB bonding have been demonstrated [136]. There are now various processes that can be exploited to avoid the inconveniences related to suspended membranes, while keeping the advantages of high vertical confinement and shallow structuring.

As in the case of nonlinear devices, the control of the Q-factor is a second important issue that was extensively considered for the optimization of the properties of a microlaser. The important results, which were obtained in Japan, by the groups of S. Noda and M. Notomi, on the possibility of achieving very low modal volume, together with high Q-factor resonators, on membranes have already been discussed in this review [96–109].

Other designs based on 2D PhC membranes have been proposed, including ultrasmall lasers, resulting from shifting two holes, as proposed by Nozaki et al. [137] in a so-called point-shift cavity design. Using such resonators, and in particular photonic heterostructures, made it possible to achieve not only very low threshold lasers, but also high Q/V ratio PhC resonators for cavity quantum electrodynamics, including single-photon sources or microlasers based on a limited number of quantum dot emitters. Such structures are considered as basic building blocks for future integrated quantum optical networks (see e. g. [138]).

At this stage, and coming back to the PhC laser vs. microlaser distinction, the approaches based on slow-light modes to reach laser emission should be mentioned. Imada et al. [139] have proposed to combine a gain material with a shallow etched PhC structure, in order to realize second-order DFB-like lasers. This important result demonstrated the possibility of obtaining surface-emitting lasers using stacks that are much simpler than in the case of VCSELs. As later demonstrated by Monat et al. [140], the gain material may be included in a fully corrugated PhC membrane bonded onto a low refractive index layer. In this paper, the authors demonstrated first-order DFB-like lasing, with in-plane light emission, potentially coupled to a planar waveguide. Another important result is that the mode localization may be very much increased in the case of such active membranes. This spatial localization is indeed proportional to the curvature of the dispersion characteristics of the Bloch

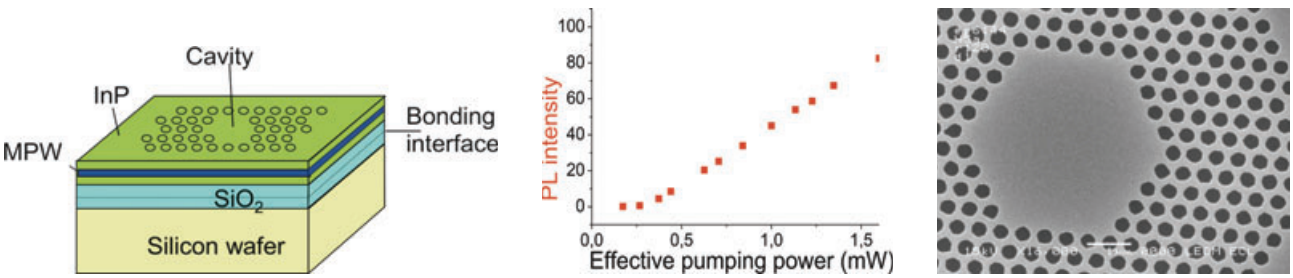

Figure 22 (online color at: www.lpr-journal.org) Hexagonal 2DPhC cavity based on an InP/SiO_2/Silicon wafer bonded heterostructure: schematic view, L-L plot and SEM view – reprinted with permission from [135].

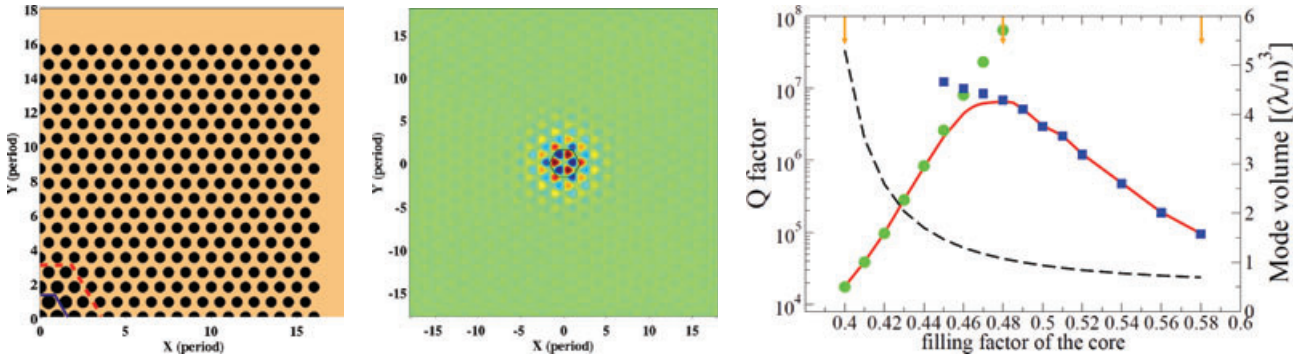

Figure 23 (online color at: www.lpr-journal.org) 2D PhC photonic heterostructure/cavity confined slow light mode. Schematic view of the resonator (one quarter of the structure is shown), H_z field for an air filling-factor (ff) of $ff = 0.48$, and calculated plots of the Q-factor (solid, red on-line, curve with peak value approaching ten million) and modal volume dependence (monotonically decreasing dashed black curve) on ff – reprinted with permission from [142].

mode, which is particularly low in the case of such structures [141]. As far as localization and optical loss control are concerned, it should be noted that laterally confining such a band-edge Bloch mode using a second PhC that exhibits a bandgap is an alternative way to build a photonic heterostructure (see Fig. 23). Such complex heterostructures were proposed – and then implemented – by Bordas et al. [142, 143], with the possibility of achieving room-temperature quantum-dot photonic crystal lasers operating at around 1.5 µm.

A key property of the PhC structure is the possibility of selecting appropriate resonant band-edge Bloch modes in such a way as to build either an inplane or a surface-emitting laser. Using well-suited lattice parameters, Raineri et al. [144], proposed a honeycomb PhC structure that exhibits laser emission in the vertical direction, with a low threshold. The possibility of stacking such PhC membranes with reflectors – in order to control both the laser threshold and the radiation pattern – can be achieved, once again thanks to the combination of technological processes like deposition or epitaxial growth of semiconductor stacks, and molecular wafer bonding. This combined vertical and lateral control of the electromagnetic field using a 2D PC combined with layer stacks will be referred to as the 2.5D approach. A whole set of active structures using this concept was investigated, and yielded important results including lasing, but also all-optical control of the Bloch resonances. These regimes were analyzed in detail in [145, 146] – for the case of a honeycomb PhC of air holes – but also, more recently, for the case of InP posts on Si/SiO_2 Bragg reflectors [147]. At this point, it should be mentioned that such quasi-3D light-control strategies enable the increase of the Q-factor of the resonator, but also the inhibition of the spontaneous emission into the radiative mode continuum. As stated in early papers on PhCs, this inhibition indeed leads to a strong decrease of the lasing threshold.

While the 2.5D approach may lead to light localization within the PhC layer, it is also possible to use a PhC membrane as a reflector, in a more compact and versatile way than the usual vertical Bragg reflectors. Indeed, the selection of the structure topography makes it possible to control the coupling efficiency between the free space and the selected guided mode resonances, and therefore the photon lifetime; the light being then reflected back into free space. Finally, light can be localized between two superimposed PhC mirrors, which may, at the same time, act as grating couplers to inject the emitted light into integrated waveguides. This illustrated the point that PhC structures, and more specifically the 2.5D approach, constitute a unique way to build bridges between free space and integrated optics.

One of the advantages of the use of PhC structures as reflectors is that the gain layer does not need to be patterned, which subsequently simplifies the optoelectronic device technology, while enabling a high kinetic lateral confinement based on slow-light processes. It remains the case that developing electrically driven PhCs to realize ultracompact laser diodes is still a challenge. The first important result was published by Park et al. [148], using a suspended membrane including support by – and current supply through – a central post, while the resonant mode was carefully selected. In a recent publication, Ellis et al. [149] successfully developed an alternative approach, forming a lateral p–i–n junction by ion implantation and thereby making it possible to electrically inject current into a quantum-dot photonic-crystal nanocavity laser in gallium arsenide (Fig. 24). Continuous-wave lasing was observed at temperatures up to 150 K, with thresholds down to 181 nA.

It is now clear that compact, electric injection-current-driven, semiconductor lasers with very low threshold current values can be realized. But alternative approaches based on plasmonic confinement [150] have the potential to compete with lasers based on photonic crystal principles – provided that the technology for electrical injection has been mastered.

11. Conclusions

This review article has been concerned with photonic crystal (PhC) devices. As has been partially demonstrated, there is by now an extensive research literature on this topic – and this review has not attempted to provide comprehensive coverage of the entire field. There is also a large area of

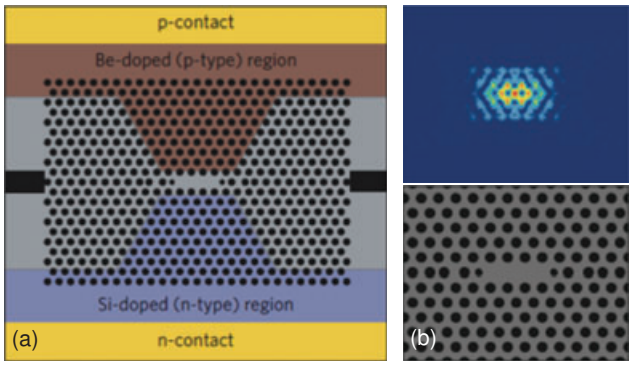

Figure 24 (online color at: www.lpr-journal.org) Design of the electrically pumped photonic-crystal laser – reprinted with permission from [149]. Copyright 2011, Nature Photonics. (a) Schematic of the electrically pumped photonic-crystal laser. The p-type doping region is indicated in red, and the n-type region in blue. The width of the intrinsic region is narrow in the cavity region to direct current flow to the active region of the laser. A trench is added to the sides of the cavity to reduce leakage current. (b) Modified three-hole defect photonic-crystal cavity design (top) and an FDTD simulation of the E-field of the cavity mode in such a structure (bottom).

photonic crystal research, such as fully three-dimensionally periodic ('3D') photonic crystals, upon which we have not even touched. Instead, attention has been focused on a limited number of topics, i. e. PhC beamsplitters, slow-light structures, micro-/nanoresonators, coupled-resonator optical waveguides (CROWs) and PhC-based semiconductor lasers – with a brief mention of the possible applications area of biosensing. An initial review, with a significantly historical aspect, has considered basic principles for photonic crystals – and we hope that it will help the reader to develop a critical appreciation of the literature – and ultimately to draw their own conclusions and act upon those conclusions.

An informed appreciation of both conceptual and practical matters will, we believe, equip the next generation of researchers in this field for the task of designing and realizing devices that exploit photonic crystal principles. It is certainly credible that this future research will operate within a scenario where devices based on photonic crystal principles – and fabricated using planar technology – will be widely used commercially, in some form of integrated photonics.

Acknowledgements. We wish to acknowledge the contribution to our published work made by many coworkers, in Glasgow, Lyon and elsewhere. Our research on photonic crystal devices has been supported in part by the EPSRC in the UK, the CNRS in France, and by the European Community.

Received: 1 December 2011, **Revised:** 1 April 2012, **Accepted:** 4 June 2012

Published online: 2 July 2012

Key words: Photonic crystal, beam-splitters, slow-light structures, micro-/nano-resonators, coupled-resonator optical waveguides (CROWs).

Richard De La Rue retired from the University of Glasgow in September 2010 and joined the Photonics Research Centre at the University of Malaya in April 2011, as Visiting Professor. His recent research has been particularly concerned with photonic crystal and photonic wire structures, waveguide micro-cavities and metamaterials. This work has evolved to include research on compact lasers, photonic-crystal LEDs and the applications of photonic crystal structures and metamaterial surfaces to bio-medical and organic sensing. Prof. De La Rue has been involved in various European Community funded collaborations and has acted as program and general co-chair for the CLEO-Europe/IQEC conferences in 2007 and 2009, as co-chair for the 'Photonic Crystal Materials and Devices' conferences at SPIE's Photonics Europe in 2004, 2006 and 2008, among others. He served as IEEE-LEOS Distinguished Lecturer for two years from 1999 and became a Fellow of the IEEE (FIEEE) in 2003; Fellow of the OSA in 2007; Fellow of the Royal Academy of Engineering (FREng) in 2002; Fellow of the Royal Society of Edinburgh (FRSE, 1989) and Fellow of the Institution of Engineering and Technology (FIET/formerly FIEE) in 1997.

Christian Seassal graduated from Institut National des Sciences Appliquées de Lyon, France, in 1993, and received the PhD Degree in Condensed Matter in 1997 from Ecole Centrale de Lyon, France. He joined the INL/CNRS, Ecole Centrale de Lyon as a CNRS Researcher in 1998. His research activities have concerned micro-opto-electro-mechanical Systems (MOEMS) based on III-V compound semiconductors. His current research interests focus on photonic crystals and nanostructures for integrated photonics, quantum photonics and photovoltaics. He is the author and coauthor of approximately 75 papers in international journals and 100 international conferences. He is an Associate Editor to Optics Express and Chairman of the SPIE Photonics Europe conference "Photonic Crystal Materials and Devices".

References

[1] E. Yablonovitch, Phys. Rev. Lett. **58**(20), 2059–2062 (1987).
[2] S. John, Phys. Rev. Lett. **58**(23), 2486–2489 (1987).
[3] V. P. Bykov, Sov. J. Quantum Electron, **4**(7), 861–871 (1975).
[4] E. Yablonovitch, Sci. Am. **285**(6), 47–55 (2001).
[5] M. Patterson, S. Hughes, S. Combrie, N. V. Q. Tran, A. De Rossi, R. Gabet, and Y. Jaouen, Phys. Rev. Lett. **102**, 253903 (2009).
[6] M. Patterson and S. Hughes, J. Opt. **12**, 104013 (2010).
[7] S. Mazoyer, J. P. Hugonin, and P. Lalanne, Phys. Rev. Lett. **103**, 063903 (2009).
[8] P. W. Anderson, Phys. Rev. **109**, 1492–1505 (1958).

[9] J. D. Joannopoulos, S. G. Johnson, J. N. Winn, and R. D. Meade, Photonic Crystals: Molding the Flow of Light, 2nd edn. (Princeton University Press, Princeton, 2008).
[10] R. M. De La Rue and S. A. De La Rue, Introduction to Photonic Crystals and Photonic Bandgaps, in: Photonic Crystals: Physics and Technology, edited by C. Sibilia, T. M. Benson, M. Marciniak, and T. Szoplik (Springer Verlag Italia, Milan, 2008), Chap. 1, pp. 7–25.
[11] P. Viktorovitch, Physics of Slow Bloch Modes and their Applications, in: Photonic Crystals: Physics and Technology, edited by C. Sibilia, T. M. Benson, M. Marciniak, and T. Szoplik (Springer Verlag Italia, Milan, 2008), Chap. 2, pp. 27–43.
[12] K. Yamada, H. Morita, A. Shinya, and M. Notomi, Opt. Commun. **198**, 395–402 (2001).
[13] D. Gerace and L. Claudio Andreani, Opt. Exp. **13**(13), 4939–4951 (2005).
[14] S. Rawal, R. K. Sinha, and R. M. De La Rue, Opt. Exp. **17**(16), 13315–13325 (2009).
[15] J. M. Pottage, E. Silvestre, and P. St. J. Russell, J. Opt. Soc. Am. A **18**, 442–447 (2001).
[16] T. F. Krauss, R. M. De La Rue, and S. Brand, Nature **383**, 699–702 (1996).
[17] X. Ao, L. Liu, L. Wosinski, and S. He, Appl. Phys. Lett. **89**, 171115 (1 to 3) (2006).
[18] T. Xu, N. Zhu, M. Y.-C. Xu, L. Wosinski, J. S. Aitchison, and H. E. Ruda, Opt. Exp. **18**(6), 5420–5425 (2010).
[19] C. L. Walker, C. D. Farmer, C. R. Stanley, and C. N. Ironside, IEE Proc.-Optoelectron. **151**(6), 502–507 (2004).
[20] L. Hvozdara, A. Lugstein, N. Finger, S. Gianordoli, W. Schrenk, K. Unterrainer, E. Bertagnolli, G. Strasser, and E. Gornik, Appl. Phys. Lett. **77**, 1241–1243 (2000).
[21] P. Pottier, S. Mastroiacovo, and R. M. De La Rue, Opt. Exp. **14**(12), 5617–5633 (2006).
[22] G. P. Nordin, S. Kim, J. Cai, and J. Jiang, Opt. Exp. **10**(23), 1334–1341 (2002).
[23] S. Kim, G. P. Nordin, J. Cai, and J. Jiang, Opt. Lett. **28**(23), 2384–2386 (2003).
[24] L. Li, G. P. Nordin, and J. M. English, Jianhua Jiang, Opt. Exp. **11**(3), 282–290 (2003).
[25] S. Kim, G. P. Nordin, J. Jiang, and J. Cai, IEEE Photon. Technol. Lett. **16**(8), 1846–1848 (2004).
[26] E. Schonbrun, Q. Wu, W. Park, T. Yamashita, and C. J. Summers, Opt. Lett. **31**(21), 3104–3106 (2006).
[27] V. Zabelin, L. A. Dunbar, N. Le Thomas, R. Houdré, M. V. Kotlyar, L. O'Faolain, and T. F. Krauss, Opt. Lett. **32**(5), 530–532 (2007).
[28] L. J. Wu, M. Mazilu, J. F. Gallet, T. F. Krauss, A. Jugessur, and R. M. De La Rue, Opt. Lett. **29**(14), 1620–1622 (2004).
[29] D. W. Prather, S. Shi, D. Pustai, C. Chen, S. Venkataraman, A. Sharkawy, G. Schneider, and J. Murakowski, Opt. Lett. **29**, 50–52 (2004).
[30] Z. Lu, S. Shi, J. Murakowski, G. Schneider, C. Schuetz, and D. Prather, Phys. Rev. Lett. **96**, 173902 (2006).
[31] P.-G. Luan and K.-D. Chang, Opt. Exp. **15**(8), 4536–4545 (2007).
[32] M. Lu, S. Liao, and Y. Huang, Appl. Opt. **49**(4), 724–731 (2010).
[33] K. S. Pennington and L. Kuhn, Opt. Commun. **3**(5), 357–359 (1971).
[34] E. Y. B. Pun, K. K. Wong, I. Andonovic, P. J. R. Laybourn, and R. M. De La Rue, Electron. Lett. **18**, 740–742 (1982).
[35] Y. B. Ovchinnikov, Opt. Commun. **220**, 229–235 (2003).
[36] J. C. Maxwell, A Treatise on Electricity and Magnetism (Clarendon Press, Oxford and Macmillan, London, 1873).
[37] R. Kompfner, The Invention of the Traveling-Wave Tube (San Francisco Press, San Francisco, 1964). (See also the websites: http://en.wikipedia.org/wiki/Rudolf_Kompfner, last modified on 15 May 2012 at 08:17, and http://en.wikipedia.org/wiki/Traveling-wave_tube, last modified on 9 May 2012 at 01:27).
[38] R. Kompfner, Rep. Prog. Phys. **15**, 275–327 (1952).
[39] J. R. Pierce, Traveling-Wave Tubes (van Nostrand Co., New York, 1950).
[40] R. H. Varian and S. F. Varian, J. Appl. Phys. **10**(5), 321–327 (1939). (See also the website at: http://en.wikipedia.org/wiki/Klystron, last modified on 5 June 2012 at 17:00).
[41] S. Ramo, Phys. Rev. **56**, 276–283 (1939).
[42] G. Convert and T. Yeou, in: Millimeter and Submillimeter Waves (Illife Books, London, 1964), Chap. 4. (See also the website at: http://en.wikipedia.org/wiki/Backwardwaveoscillator, last modified on 27 January 2012 at 18:35).
[43] G. Kantorowicz and P. Palluel, Backward Wave Oscillators, in: Infrared and Millimeter Waves, Vol. 1, edited by K. Button (Academic Press, New York, 1979), Chap. 4.
[44] G. Adamo, K. F. MacDonald, Y. H. Fu, C.-M. Wang, D. P. Tsai, F. J. Garcia de Abajo, and N. I. Zheludev, Phys. Rev. Lett. **103**, 113901-1–4 (2009).
[45] G. Adamo, K. F. MacDonald, Y. H. Fu, D. P. Tsai, F. J. Garcia de Abajo, and N. I. Zheludev, J. Opt. **12**, 024012-1 to -5 (2010).
[46] S. J. Smith and E. M. Purcell, Phys. Rev. **92**, 1069 (1953).
[47] A. Gover and A. Yariv, Appl. Phys. **16**, 121–138 (1978).
[48] A. Talneau, J. Opt. **12**, 104005 (7 pp.) (2010).
[49] L. H. Frandsen, A. V. Lavrinenko, J. Fage-Pedersen, and P. I. Borel, Opt. Exp. **14**, 9444–9450 (2006).
[50] A. Yu. Petrov and M. Eich, Appl. Phys. Lett. **85**(21), 4866–4868 (2004).
[51] S. Rawal, R. K. Sinha, and R. M. De La Rue, IEEE J. Light Wave Technol. **28**(17), 2560–2571 (2010).
[52] T. F. Krauss, Nature Photon. **2**, 448–450 (2008).
[53] I. Ntakis, P. Pottier, and R. M. De La Rue, J. Appl. Phys. **96**(1), 12–18 (2004).
[54] D. M. Beggs, T. P. White, L. Cairns, L. O'Faolain, and T. F. Krauss, IEEE Photon. Technol. Lett. **21**(1), 24–26 (2009).
[55] E. A. Camargo, H. M. H. Chong, and R. M. De La Rue, Appl. Opt. **45**(25), 6507–6510 (2006).
[56] E. A. Camargo, H. M. H. Chong, and R. M. De La Rue, Opt. Exp. **12** (4), 588–592 (2004).
[57] E. A. Camargo, H. M. H. Chong, and R. M. De La Rue, Photon. Nanostruct.-Fundamen. Appl. **2**(3), 207–213 (2004).
[58] A. Melloni, A. Canciamilla, C. Ferrari, F. Morichetti, L. O'Faolain, T. Krauss, R. M. De La Rue, A. Samarelli, and M. Sorel, IEEE Photon. J. **2**(2), 181–194 (2010).
[59] F. Morichetti, A. Canciamilla, M. Martinelli, A. Melloni, A. Samarelli, R. M. De La Rue, and M. Sorel, Appl. Phys. Lett. **96**, 081112-1–3 (2010).
[60] H. M. H. Chong and R. M. De La Rue, IEEE Photon. Technol. Lett. **16**(6), 1528–530 (2004).
[61] Y. A. Vlasov, M. O'Boyle, H. F. Hamann, and S. J. McNab, Nature **438**, 65–69 (2005).

[62] J.-M. Brosi, C. Koos, L. C. Andreani, M. Waldow, J. Leuthold, and W. Freude, Opt. Exp. **16**, 4177–4191 (2008).
[63] J. Wülbern, J. Hampe, A. Petrov, M. Eich, J. Luo, A. Jen, A. Falco, T. Krauss, and J. Bruns, Appl. Phys. Lett. **94**(24), 241107 (2009).
[64] A. Baron, A. Ryasnyanskiy, N. Dubreuil, P. Delaye, Q. V. Tran, S. Combrié, A. De Rossi, R. Frey, and G. Roosen, Opt. Exp. **17**(2), 552–557 (2009.
[65] K. Ikeda and Y. Fainman, Solid-State Electron. **51**, 1376–1380 (2007).
[66] K. Inoue, H. Oda, N. Ikeda, and K. Asakawa, Opt. Exp. **17**, 7206–7216 (2009).
[67] S. Rawal, R. K. Sinha, and R. M. De La Rue, Impact of slow light on nonlinear phase sensitivity in SOI photonic crystals, in: Proceedings of Photonics 2010, IIT Guwahati, India, 11th–15th December (2010).
[68] C. Monat, W. Corcoran, M. Ebnali-Heidari, C. Grillet, B. J. Eggleton, T. P. White, L. O'Faolain, and T. F. Krauss, Opt. Exp. **17**(4), 2944–2953 (2009).
[69] C. Monat, W. Corcoran, D. Pudo, M. Ebnali-Heidari, C. Grillet, M. D. Pelusi, D. J. Moss, B. J. Eggleton, T. P. White, L. O'Faolain, and T. F. Krauss, IEEE J. Selec. Top. Quantum Electron. **16**(1), 344–355 (2010).
[70] P. Pottier, M. Gnan, and R. M. De La Rue, Opt. Exp. **15** (11), 6569–6575 (2007).
[71] P. Pottier, I. Ntakis, and R. M. De La Rue, Opt. Commun. **223**(4–6), 339–347 1st Aug (2003).
[72] K. L. Tsakmakidis, A. D. Boardman, and O. Hess, Nature **450**, 397–401 (2007).
[73] A. Reza, M. M. Dignam, and S. Hughes, Nature **455**, E10–E11 (2008).
[74] R. E. Collin, Field Theory of Guided Waves, 2nd edn. (IEEE Press, New York, 1991).
[75] P. Velha, J. P. Hugonin, and P. Lalanne, Opt. Exp. **15**(10), 6102–6112 (2007).
[76] J. P. Hugonin, P. Lalanne, T. P. White, and T. F. Krauss, Opt. Lett. **32**(18), 2638–2640 (2007).
[77] T. P. White, L. C. Botten, C. Martijn de Sterke, K. B. Dossou, and R. C. McPhedran, Opt. Lett. **33**(22), 1644–2646 (2008).
[78] J. S. Foresi, P. R. Villeneuve, J. Ferrera, E. R. Thoen, G. Steinmeyer, S. Fan, J. D. Joannopoulos, L. C. Kimerling, H. I. Smith, and E. P. Ippen, Nature **390**, 143 (1997).
[79] J. C. Chen, S. Fan, P. R. Villeneuve, and J. D. Joannopoulos, IEEE J. Lightwave Technol. **14**(11), 2575–2580 (1996).
[80] P. R. Villeneuve, S. Fan, J. D. Joannopoulos, K.-Y. Lim, G. S. Petrich, L. A. Kolodziejski, and R. Reif, Appl. Phys. Lett. **67**(2), 167–169 (1995).
[81] K.-Y. Lim, D. J. Ripin, G. S. Petrich, L. A. Kolodziejski, E. P. Ippen, M. Mondol, H. I. Smith, P. R. Villeneuve, S. Fan, and J. D. Joannopoulos, J. Vac. Sci. Technol. B **17**(3), 1171–1174 (1999).
[82] A. S. Jugessur, P. Pottier, and R. M. De La Rue, Electron. Lett. **39**(4), 367–369 (2003).
[83] A. S. Jugessur, P. Pottier, and R. M. De La Rue, Opt Exp. **12**(7), 1304–1312 (2004).
[84] T. F. Krauss, B. Vögele, C. R. Stanley, and R. M. De La Rue, IEEE Photon. Technol. Lett. **9**, 176–178 (1997).
[85] T. F. Krauss, O. Painter, A. Scherer, J. S. Roberts, and R. M. De La Rue, Opt. Eng. **37**(4), 1143–1148 (1998).
[86] L. Raffaele, R. M. De La Rue, J. S. Roberts, and T. F. Krauss, IEEE Photon. Technol. Lett. **13**(3), 176–178 (2001).
[87] L. Raffaele, R. M. De La Rue, and T. F. Krauss, Opt. Quantum Electron. **34**(1–3), 101–111 (2002).
[88] T. D. Happ, M. Kamp, and A. Forchel, Opt. Quantum Electron. **34**, 91–99 (2002).
[89] G. Erwin, A. C. Bryce, and R. M. De La Rue, Proc. SPIE **5958**, 59580E (2005); doi:10.1117/12.622969.
[90] P. Millar, N. G. R. Broderick, D. J. Richardson, J. S. Aitchison, R. M. De La Rue, and T. F. Krauss, Opt. Lett. **24**, 685–687 (1999).
[91] P. Millar, N. G. R. Broderick, D. J. Richardson, J. S. Aitchison, R. M. De La Rue, and T. F. Krauss, Opt. Photon. News **10** (12), 43–44 (1999).
[92] N. G. R. Broderick, P. Millar, D. J. Richardson, J. S. Aitchison, R. De La Rue, and T. Krauss, Opt. Lett. **25**(10), 740–742 (2000).
[93] C. J. M. Smith, T. F. Krauss, R. M. De La Rue, D. Labilloy, H. Benisty, C. Weisbuch, U. Oesterle, and R. Houdré, IEE Proc.-Optoelectron. **145**(6), 373–378 (1998).
[94] C. J. M. Smith, H. Benisty, D. Labilloy, U. Oesterle, R. Houdré, T. F. Krauss, R. M. De La Rue, and C. Weisbuch, Electron. Lett. **35**, 228–230 (1999).
[95] C. J. M. Smith, R. M. De La Rue, M. Rattier, S. Olivier, H. Benisty, C. Weisbuch, T. F. Krauss, R. Houdre, and U. Oesterle, Phys. Lett. **78**(11), 1487–1489 (2001).
[96] Y. Akahane, T. Asano, B.-S. Song, and S. Noda, Nature **425**, 944–947 (2003).
[97] B.-S. Song, S. Noda, T. Asano, and Y. Akahane, Nature Mater. **4**, 207–210 (2005).
[98] Y. Takahashi, H. Hagino, Y. Tanaka, B. S. Song, T. Asano, and S. Noda, Opt. Exp. **15**, 17206–17213 (2007).
[99] H.-Y. Ryu, M. Notomi, and Y.-H. Lee, Appl. Phys. Lett. **83**, 4294–4296 (2003).
[100] E. Kuramochi, M. Notomi, S. Mitsugi, A. Shinya, T. Tanabe, and T. Watanabe, Appl. Phys. Lett. **88**, 041112 (2006).
[101] T. Tanabe, M. Notomi, E. Kuramochi, A. Shinya, and H. Taniyama, Nature Photon. **1**, 49–52 (2007).
[102] T. Uesugi, B. Song, T. Asano, and S. Noda, Opt. Exp. **14**, 377–386 (2006).
[103] W. C. Stumpf, M. Fujita, M. Yamaguchi, T. Asano, and S. Noda, Appl. Phys. Lett. **90**, 231101 (2007).
[104] T. Tanabe, K. Nishiguchi, A. Shinya, E. Kuramochi, H. Inokawa, and M. Notomi, Appl. Phys. Lett. **90**, 031115 (2007).
[105] L.-D. Haret, T. Tanabe, E. Kuramochi, and M. Notomi, Opt. Exp. **17**(23), 21108–21117 (2009).
[106] M. Notomi and H. Taniyama, Opt. Exp. **16**(23), 18657–18666 (2008).
[107] J. Upham, Y. Tanaka, T. Asano, and S. Noda, Opt. Exp. **16**(26), 21721–21730 (2008).
[108] M. Nomura, N. Kumagai, S. Iwamoto, Y. Ota, and Y. Arakawa, Opt. Exp. **17**(18), 15975–15982 (2009).
[109] M. Nomura, K. Tanabe, S. Iwamoto, and Y. Arakawa, Opt. Exp. **18**(8), 8144–8150 (2010).
[110] P. Velha, J. C. Rodier, P. Lalanne, J. P. Hugonin, D. Peyrade, E. Picard, T. Charvolin, and E. Hadji, New J. Phys. (IOP) **8**(204), 1–13 (2006).
[111] P. Velha, E. Picard, T. Charvolin, E. Hadji, J. Rodier, P. Lalanne, and D. Peyrade, Opt. Exp. **15**, 16090 (2007).
[112] A. R. Md Zain, M. Gnan, H. M. H. Chong, M. Sorel, and R. M. De La Rue, IEEE Photon. Technol. Lett. **20**(1), 6–8 (2008).
[113] A. R. Md Zain, N. P. Johnson, M. Sorel, and R. M. De La Rue, Opt. Exp. **16**(16), 12084–12089 (2008).

[114] A. R. Md Zain, N. P. Johnson, M. Sorel, and R. M. De La Rue, IEEE Photon. Technol. Lett. **21**(24), 1789–1791 (2009).
[115] M. Belotti, M. Galli, D. Gerace, L. Andreani, G. Guizzetti, A. R. Md Zain, N. P. Johnson, M. Sorel, and R. M. De La Rue, Opt. Exp. **18**(2), 1450–1461 (2010).
[116] F. Morichetti, C. Ferrari, A. Canciamilla, and A. Melloni, Laser Photon. Rev. DOI: 10.1002/lpor.201100018, available online 13 September (2011).
[117] A. Melloni, A. Canciamilla, C. Ferrari, F. Morichetti, L. O'Faolain, T. Krauss, R. M. De La Rue, A. Samarelli, and M. Sorel, IEEE Photon. J. **2**(2), 181–194 (2010).
[118] F. Morichetti, A. Canciamilla, C. Ferrari, A. Samarelli, M. Sorel, and A. Melloni, Nature Commun. 2:296 DOI: 10.1038/ncomms1294, 3 May (2011).
[119] M. L. Cooper, G. Gupta, M. A. Schneider, W. M. J. Green, S. Assefa, F. Xia, Y. A. Vlasov, and S. Mookherjea, Opt. Exp. **18**(25), 26505–26516 (2010).
[120] F. Xia, L. Sekaric, and Y. Vlasov, **1**, 65–71 (2007).
[121] A. Yariv, Y. Xu, R. K. Lee, and A. Scherer, Opt. Lett. **24**, 711–713 (1999).
[122] C. Jin, N. P. Johnson, H. M. H. Chong, A. S. Jugessur, S. Day, D. Gallagher, and R. M. De La Rue, Opt. Exp. **13**(7), 2295–2302 (2005).
[123] D. O'Brien, M. D. Settle, T. Karle, A. Michaeli, M. Salib, and T. F. Krauss, Opt. Exp. **15**(3), 21721–21730 (2007).
[124] A. S. Jugessur, P. Pottier, and R. M. De La Rue, Photon. Nanostruct. Fundam. Appl. **3**(1), 25–29 (2005).
[125] A. R. Md Zain, N. P. Johnson, M. Sorel, and R. M. De La Rue, Electron. Lett. **45**(5), 283–284 (2009).
[126] M. Notomi, E. Kuramochi, and T. Tanabe, Nature Photon. **2**(12), 741–747 (2008).
[127] R. M. De La Rue, Nature Photon. **2**(12), 715–716 (2008).
[128] A. Melloni and F. Morichetti, Nature Photon. **3**(3), 119 (2009).
[129] J. Cooper, A. Glidle, and R. De La Rue, Opt. Photon. News **21**(9), 26–31 (2010).
[130] E. Chow, A. Grot, L. W. Mirkarimi, M. Sigalas, and G. Girolami, Opt. Lett. **29**(10), 1093–1095 (2004).
[131] F. Dortu, H. Egger, K. Kolari, T. Haatainen, P. Furjes, Z. Fekete, D. Bernier, G. Sharp, B. Lahiri, S. Kurunczi, J.-C. Sanchez, N. Turck, P. Petrik, D. Patko, R. Horvath, S. Eiden, T. Aalto, S. Watts, N. P. Johnson, R. M. De La Rue, and D. Giannone, Proc. SPIE **8087**, 80870D (2011); doi:10.1117/12.889420.
[132] A. Densmore, D.-X. Xu, S. Janz, P. Waldron, T. Mischki, G. Lopinski, A. Delâge, J. Lapointe, P. Cheben, B. Lamontagne, and J. H. Schmid, Opt. Lett. **6**, 596–598 (2008).
[133] D.-X. Xu, A. Densmore, A. Delâge, P. Waldron, R. McKinnon, S. Janz, J. Lapointe, G. Lopinski, T. Mischki, E. Post, P. Cheben, and J. H. Schmid, Opt. Exp. **16**(19), 15137–15148 (2008).
[134] O. Painter, R. K. Lee, A. Scherer, A. Yariv, J. D. O'Brien, P. D. Dapkus, and I. Kim, Science **284**(5421), 1819–1821 (1999).
[135] C. Monat, C. Seassal, X. Letartre, P. Viktorovitch, P. Regreny, M. Gendry, P. Rojo-Romeo, G. Hollinger, E. Jalaguier, S. Pocas, and B. Aspar, Electron. Lett. **37**, 764 (2001).
[136] Y. Halioua, A. Bazin, P. Monnier, T. J. Karle, G. Roelkens, I. Sagnes, R. Raj, and F. Raineri, Opt. Exp. **19**, 9221–9231 (2011).
[137] K. Nozaki, S. Kita, and T. Baba, Opt. Exp. **15**, 7506–7514 (2007).
[138] A. Faraon, A. Majumdar, D. Englund, E. Kim, M. Bajcsy, and J. Vuckovic, New J. Phys. **13**, 055025 (2011).
[139] M. Imada, A. Chutinan, S. Noda, and M. Mochizuki, Phys. Rev. B **65**, 195306 (2002).
[140] C. Monat, C. Seassal, X. Letartre, P. Regreny, M. Gendry, P. Rojo-Romeo, P. Viktorovitch, M. Le Vassor d'Yerville, D. Cassagne, J. P. Albert, E. Jalaguier, S. Pocas, and B. Aspar, Appl. Phys. Lett. **81**, 5102–5104 (2002).
[141] X. Letartre, J. Mouette, J.-L. Leclercq, P. Rojo-Romeo, C. Seassal, and P. Viktorovitch, J. Lightwave Technol. **21**, 1691–1699 (2003).
[142] F. Bordas, M. J. Steel, C. Seassal, and A. Rahmani, Opt. Exp. **15**, 10890–10902 (2007).
[143] F. Bordas, C. Seassal, E. Dupuy, P. Regreny, M. Gendry, P. Viktorovitch, M. J. Steel, and A. Rahmani, Opt. Exp. **17**, 5439–5445 (2009).
[144] F. Raineri, C. Cojocaru, P. Monnier, A. Levenson, R. Raj, C. Seassal, X. Letartre, and P. Viktoravitch, Appl. Phys. Lett. **85**, 1880–1882 (2004).
[145] A. M. Yacomotti, F. Raineri, G. Vecchi, R. Raj, A. Levenson, B. Ben Bakir, C. Seassal, X. Letartre, P. Viktorovitch, L. Di Cioccio, and J. M. Fedeli, Appl. Phys. Lett. **88**, 231107 (2006).
[146] L. Ferrier, O. El Daif, X. Letartre, P. Rojo Romeo, C. Seassal, R. Mazurczyk, and P. Viktorovitch, Opt. Exp. **17**, 9780–9788 (2009).
[147] C. Sciancalepore, B. Ben Bakir, X. Letartre, J.-M. Fedeli, N. Olivier, D. Bordel, C. Seassal, P. Rojo-Romeo, P. Regreny, and P. Viktorovitch, J. Lightwave Technol. **29**, 2015–2024 (2011).
[148] H.-G. Park, S.-H. Kim, S.-H. Kwon, Y.-G. Ju, J.-K. Yang, J.-H. Baek, S.-B. Kim, and Y.-H. Lee, Science **305**, 1444–1447 (2004).
[149] B. Ellis, M. Mayer, G. Shambat, T. Sarmiento, E. Haller, J. S. Harris, and J. Vuckovic, Nature Photon. **5**, 297–300 (2011).
[150] M. Khajavikhan, A. Simic, M. Katz, J. H. Lee, B. Slutsky, A. Mizrahi, V. Lomakin, and Y. Fainman, Nature **482**, 204–207 (2012).